T.C.
MARMARA UNIVERSITY
INSTITUTE FOR GRADUATE STUDIES IN
PURE AND APPLIED SCIENCES

OPTIMIZATION OF THE CONTINUOUS STAGEWISE PROCESSES AND OPTIMAL USE OF AIR AND FUEL ALONG THE TUNNEL KILN BRICK MAKING PROCESS

Sinem KAYA
(Chemical Engineering)
(141103320040052)

THESIS
FOR THE DEGREE OF MASTER OF SCIENCE
IN
CHEMICAL ENGINEERING PROGRAMME

SUPERVISORS

Asst. Prof. Dr. Kurtul KÜÇÜKADA

Asst. Prof. Dr. Ebru MANÇUHAN

ISTANBUL 2007

ACKNOWLEDGEMENTS

First and foremost I wish to thank my supervisor, Asst. Prof. Dr. Kurtul KÜÇÜKADA. I would like to express my deep and sincere gratitude to him for his help, simulating suggestions and encouragement in all the time of research for and writing of this thesis. His wide knowledge and his logical way of thinking have been of great value for me. His personal guidance has provided a good basis for the present thesis. I could not have imagined having a better supervisor and without his common-sense, knowledge, perceptiveness I would never have finished.

I am deeply grateful to my other supervisor, Asst. Prof. Dr. Ebru Mançuhan for her detailed and constructive comments, corrections and for her important support and help in bringing this thesis to completion.

I wish to express my love and gratitude to all my family who gave me emotional and economical support throughout all my educational life.

And last but not least, I would like to thank Murat for his love, understanding and support and for the incredible amount of patience he had with me in the last two years.

26.06.2007 Sinem KAYA

CONTENTS

ABSTRACT

OPTIMIZATION OF THE CONTINUOUS STAGEWISE PROCESSES AND OPTIMAL USE OF AIR AND FUEL ALONG THE TUNNEL KILN BRICK MAKING PROCESS

This thesis dealt with the optimization of tunnel kiln brick making process. Due to the dynamic characteristics, tunnel kiln which consists of three different separate zones namely; preheating, firing and cooling was optimized by using a model based optimization technique. The optimization was realized by considering each zone as a decomposable structured system formed of N interconnected cells.

A mathematical model representing the phenomena of heat transfer and fluid flow was developed to compute the state variables such as the air mass flow rate, brick and air temperatures along the cooling zone of a tunnel kiln. Using the mathematical model, the optimization of the cooling zone was performed to minimize the pressure drop by finding the optimum suction and blowing air flow rate profiles in addition to the ambient air flow rate entering from the brick exit side. The plant data were used to compare with the model-based optimization results. The results showed that the minimum pressure drop was obtained by considering the tunnel kiln cooling zone composed of two regions of suction and two regions of blowing while satisfying the process constraints.

The objective function of the firing zone is the minimum fuel cost. When the developed model equations were solved for the minimum fuel cost by satisfying process constraints, optimal operating conditions in terms of the optimal flow rate of the pulverized coal, admixed coal within the bricks and flow rate of the secondary air fed from top of the kiln were obtained. The constraints to be satisfied are the admixed coal within the brick body and the carbon percentage in the brick body. Admixed and pulverized coals were used as the energy suppliers to the system and secondary air supplied into the tunnel kiln was used for complete combustion of

admixed coal particles and pulverized coal, and for strength development. Optimization results show that using more admixed coal, while keeping the carbon percentage in the brick constant, decreases the amount of pulverized coal, and thus reduces the fuel cost.

Keywords: Tunnel kiln, optimization, heat transfer, pressure drop, cooling zone, firing zone

06/2007 **Sinem Kaya**

ÖZET

SÜREKLİ KADEMELİ PROSESLERİN OPTİMİZASYONU VE TÜNEL FIRIN TUĞLA ÜRETİMİNDE FIRIN BOYUNCA EN UYGUN HAVA VE YAKIT KULLANIMININ BULUNMASI

Bu tezde tünel fırın tuğla üretiminin optimizasyonu yapıldı. Ön ısıtma, pişirme ve soğutma olmak üzere üç bölümden oluşan tünel fırının optimizasyonu, dinamik yapısı nedeni ile model bazlı optimizasyon tekniği geliştirilerek yapıldı. Optimizasyon yapılırken, pişirme ve soğutma bölgelerinin, birbirine bağlı N sayıda ayrılabilir yapıda hücrelerden oluştuğu varsayıldı.

Isı transferi ve akışkan akımına dayalı model denklemler tünel fırın soğutma bölgesi boyunca hava debisi, tuğla ve hava sıcaklıkları gibi sistem durum değişkenlerini bulmak için geliştirildi. Soğutma bölgesinde basınç kaybını minimum yapmak için, matematiksel denklemler kullanılarak emilen ve beslenen hava debi profilleri ile tuğla çıkış bölgesinden giren hava debisinin optimum değerleri bulunarak soğutma bölgesinin optimizasyonu gerçekleştirildi. Fabrika verileri ile optimizasyon sonuçları karşılaştırıldı. Optimizasyon sonuçları gösterdi ki; proses kısıtlarının sağlanarak minimum basınç kaybı elde edilmesi için tünel fırın soğutma bölgesinde iki bölgede emme ve iki bölgede de besleme yapılması gerekir.

Pişirme bölgesinin amaç fonksiyonu yakıt maliyetinin minimum olmasıdır. Geliştirilen denklemler, proses kısıtları sağlanarak, minimum yakıt maliyeti için çözüldüğünde, püskürtme kömür ve tuğla iç kömür debilerinin optimum değerleri ile üst besleme havasının optimum değerleri bulundu. Pişirme bölgesinde kullanılan iç kömür ve toz kömür sistemin enerji kaynağı olarak kullanılırken tünel fırına beslenen hava da iç kömür ve püskürtme kömürün tamamen yanmasını sağlayarak tuğlaların mukavemetini arttırır.

Sonuç olarak optimizasyon sonuçları gösterdi ki; tuğla içindeki karbon yüzdesi sabit tutularak daha fazla iç kömürü kullanıldığında sisteme gerekli püskürtme kömür miktarı azalır bu da yakıt maliyetini düşürür.

Anahtar Kelimeler: Tünel fırın, optimizasyon, soğutma bölgesi, pişirme bölgesi

06/2007 **Sinem KAYA**

CLAIM FOR ORIGINALITY

OPTIMIZATION OF THE CONTINUOUS STAGEWISE PROCESS AND OPTIMAL USE OF AIR AND FUEL ALONG THE TUNNEL KILN BRICK MAKING PROCESS

Dynamic optimization has become an increasingly important aspect in the industrial processes due to the dynamic structure of plant operations. In this thesis, developed model based equations to obtain optimal policies were solved by using numerical methods for the optimization of cooling and firing zones of the tunnel kiln.

In this study, dynamic behavior of the tunnel kiln was taken into account to find the minimum pressure drop throughout the cooling zone while satisfying an efficient heat recovery from the brick and the minimum fuel cost by finding the optimal flow rate of the pulverized coal, admixed coal within the bricks in addition to flow rate of the secondary air throughout the firing zone.

The objective function for the cooling zone is the pressure drop along the cooling zone. Pressure drop is a function of the flow rate of the air passing through the cooling zone and temperature of the air. Fresh air entering at the cooling exit side, the suction and blowing air flow rates were optimized by satisfying process constraints in order to increase the heat transfer between the bricks and air while minimizing the total pressure drop.

Our objective in the firing zone is to make the fuel cost minimum. The combustion of admixed coal particles with the diffused oxygen into the bricks and the reaction of the pulverized coal introduced at the top of kiln with the oxygen of fresh air were evaluated by solving the developed model equations for each Δx element along the firing zone to find the minimum fuel cost.

06/2007 **Asst.Prof. Dr. Kurtul KÜÇÜKADA** **Sinem KAYA**
Asst. Prof. Dr. Ebru MANÇUHAN

LIST OF SYMBOLS

a	heat transfer area per unit volume of bricks (m^2/m^3)
C	concentration (mol/m^3)
$\mathbf{C_p}$	heat capacity (kJ/kg °C)
$\mathbf{D_{eq}}$	equivalent diameter (m)
e	void fraction (-)
E	modulus of elasticity (kPa)
f	friction factor
F	view factor
$\mathbf{g_{ac}}$	superficial mass flow rate of admixed coal (kg/m^2s)
$\mathbf{g_b}$	superficial mass flow rate of blown air (kg/m^2s)
G	superficial mass flow rate (kg/m^2s)
$\mathbf{G_b}$	superficial mass flow rate of brick (kg brick/m^2s)
h	convective heat transfer coefficient (kJ/m^2 s °C)
J	fuel cost (Euros/kg)
k	thermal conductivity (kJ/ms°C)
K	reaction rate constant (1/s)
$\overline{L}$	dimensionless length (%)
MW	molecular weight (kg / kmol)
$\dot{m}$	mass flow rate ratio (kg/kg brick)
$\dot{\phi}_{dry}$	heat required in the drying kiln (kJ/kg brick)
s	compressive strength (kPa)
T	temperature (°C)
v	velocity (m/s)
y	mol fraction (-)
$\mathbf{w_C}$	weight fraction of carbon (kg carbon / kg brick)

Greek Letters

α_T thermal expansion coefficient (1/°C)

ΔP pressure drop (N/m^2)

ε emissivity

ρ density (kg/m^3)

σ Stefan-Boltzman coefficient ($kJ/m^2\ K^4$)

$\dot{\theta}_{max}$ maximum cooling rate of bricks (°C/s)

Subscripts

a air

b brick

bw brick packages to kiln wall

c convective

i the cell number

m measured

N total number of cells

r radiative

w wall

Superscripts

b blowing

s suction

Dimensionless groups

Nu Nusselt number

Pr Prandtl number

Re Reynolds number

LIST OF FIGURES

LIST OF TABLES

PART I

INTRODUCTION

Tunnel kilns are widely used kilns in industry for clay brick making process. The brick to be burned are stacked on flat cars which move very slowly through various temperature zones (preheating, firing and cooling) as they travel through the tunnel kiln. This process operating continuously involves the counter current flow of brick loads and air. The temperature profiles in each zone are carefully controlled. The air is supplied into the tunnel kiln at several locations to satisfy the temperature profile necessary for evaporation of bound water, for combustion of admixed and pulverized coals and for strength development.

Many researches, each one approaches from a different point of view, have been done about tunnel kiln so far. In this study, dynamic behavior of the tunnel kiln was taken into account to find the minimum pressure drop throughout the tunnel kiln while satisfying an efficient heat recovery from the brick. This dynamic structure is caused by the sucked and blown air and combustion reactions of pulverized and admixed coals. Additionally, heat transfer reactions between brick and air take a role in that dynamic structure. As a result, a dynamic optimization approach was developed to find out the optimal flow rates and locations of the suction and blowing air for minimum pressure drop and maximum heat recovery. Optimization variables and constraints change with position for the considered system due to the varying air flow rate. Therefore, the changes in their values as a function of distance were investigated along the tunnel kiln.

I.1 OBJECTIVE OF THE PRESENT WORK

In this present work, the scope was to optimize the stage-wise processes of the tunnel kiln namely cooling, firing and preheating by developing model equations

while satisfying process constraints. In this way, the optimal flow rates and locations of the suction and blowing air for sufficient heat recovery and minimum pressure drop for throughout the tunnel kiln were involved. In addition, temperature profiles of brick and air and superficial mass flow rate of air along the tunnel kiln were obtained.

The pressure drop in tunnel kiln occurs due to the flow of air through the holes of the brick and through the spacing between brick packages. During these calculations, the air flow was considered to be similar to the flow of fluids in parallel pipes. So the flow rates through the brick and spacing are different but the pressure drop through either bricks or spacing is the same. In the present work, the optimal air flow rate generated due to suction and blowing at different locations were computed to minimize the pressure drop along the cooling zone while maximizing the heat recovered.

I.2 THESIS OUTLINE

A general explanation about the process of brick making, structure of tunnel kiln and finally, objective of the present work were defined shortly in chapter 1.

Chapter II introduces the brickmaking method. This chapter is divided into three sections. In section II.1, raw materials and their chemical compositions in general are explained. In section II.2, how the materials take the brick shape is described under the heading of molding and drying. Types of the firing furnaces are gone on to outline in section II.3.

In chapter III, the operating principles and characteristics of the tunnel kiln is mentioned. The parts of this kiln, which are preheating, firing and cooling, are introduced in details in the sections of this chapter.

Chapter IV approaches from the perspective of scientific studies. It discusses existing researches concerning modeling and optimization of tunnel kiln furnaces, heat transfer phenomena and finally combustion of admixed and pulverized coals.

Chapter V presents modeling and optimization of the tunnel kiln. For simplicity and getting general information, the first section starts with macroscopic mass and energy balances. Modeling of heat transfer and combustion is described in the following section. It includes convective heat transfer, radiation and combustion of coal as a function of distance in the firing zone. Combustion of coal is examined

in two parts as combustion of admixed and pulverized coal and diffusion of oxygen within the bricks. Section V.3 is based on the air flow and pressure drop while evaporation of bound water in the preheating zone is reported in section V.4. The last section covers optimization that expresses cooling, firing and preheating separately.

Chapter VI, the last section, includes results and discussion. Industrial data taken from the related factory is tabulated in the first section of this chapter. Then, for each zone, overall mass and energy balances are investigated separately. Finally, lengthwise optimization of the tunnel kiln are taken into consideration and each zone as in the previous section is evaluated separately again.

PART II

BRICKMAKING

Brick, which is a construction material, is manufactured by exposing molds, formed of clay and sand to high temperature treatment. Although the basic steps of brick manufacturing remain standard throughout the years, more complete knowledge of the characteristics of the raw materials, improved kiln designs and controlled heat in the kilns have resulted minor variations in brickmaking process from day to day. Essentially, brick is produced by mixing clay with water, forming them into desired shapes, then drying and firing them. The basic step firing causes the clay particles to develop physically and chemically solid bonds together to create extremely durable building material. Furthermore, during the last century, technological developments have helped to make brick manufacturing a very efficient and highly productive process while retaining a high quality for the final product.

II.1 RAW MATERIALS AND THEIR CHEMICAL COMPOSITION

Composition and characteristics of the raw materials directly affect the properties of brick. Therefore, the physical and chemical properties of raw materials should be analyzed in order to produce bricks with desired qualities such as strength, density, thermal expansion. The final properties of bricks are determined by the properties of the raw materials used in addition to the heat treatment process in the tunnel kiln. Materials used and their functions for brick making can be seen in Table II.1.

The basic raw material of brick is clay, which is one of the most abundant mineral on earth. Chemically, it is composed of silica and alumina with varying amounts of metallic oxides and other impurities. Although technically metallic oxides are impurities, they act as fluxes, promoting fusion at lower temperatures. Metallic oxides (iron, magnesium and calcium) influence the color of the finished fired product.

Clay used in the production of brick must possess some specific properties and characteristics. To satisfy modern production requirements, clays must have plasticity, which permits them to be shaped or molded when mixed with water; and they must have sufficient wet and air-dried tensile strength to maintain their shape after forming. In addition, when subjected to elevated temperatures, the clay particles must fuse together.

The other raw material is sand (silicon oxide) which can be used to make minor adjustment to the quality of basic materials. It can be added to basic raw materials to prevent the brick from becoming too brittle, while drying. Sand can also be used as a stabilizer in a mixture. Another important use of sand is in the brickmaking process, where it is used to keep the bricks from sticking to the molds.

Iron oxide (Fe_2O_3) and aluminum oxide (Al_2O_3), both exist in clay and sand in varying amounts, are another important ingredients. While the former gives the red color, durability and hardness to the brick, the latter is used to make the color lighter and brighter.

Usually low calorific value coal is used as an additive in brick in order to reduce the fuel cost and increasing the bond uniformity and porosity.

Table II.1 Materials Used and Their Functions for Brick Making

Materials	Functions
Clay (Bentonite, Alumina, Al_2O_3)	Plasticity and bonding
Sand (SiO_2)	Bonding and reducing the cost
Coal (Carbon)	Reducing the energy requirement, increasing the porosity and bonding uniformity.

It is impossible to give a typical composition for clay, since the percentages of the different constituents vary through such wide ranges as illustrated in Table II.2.

Table II.2 Chemical Composition of Clay and Sand

	Clay (%)	Sand (%)
SiO_2	66-50	≅ 98
Al_2O_3	21-32	0.3-1.5
Fe_2O_3	2-6	0.04-0.07
Lost on ignition	6.5-12.5	0.2

II.2 MOULDING AND DRYING

The next step after mixing all the raw materials with water is to make the material into the shape of brick. The mixture is sent to a machine which presses the wet mix into molds. Then they are placed on pallets and allowed to dry.

When bricks come from molding, they contain about 20-30 percent moisture due to the water added during clay preparation to increase workability of the mixture. Before the firing process begins, most of this free water is evaporated slowly in dryer at temperatures ranging from about 38°C to 204°C for mainly two reasons. First, there will be less cracking in fired bricks with less water content. Second, drying is established by the hot air coming from the cooling zone so that energy used in the firing zone will be reduced and more heat will be recovered.

II.3 FIRING FURNACES

Firing furnaces based on the working principles can be categorized into two groups; continuous and periodic (batch) kilns. Continuous kilns are best for consistent, high volume production. They are more fuel efficient than periodic kilns, since only the product and kiln furniture must be heated. It is easier to achieve uniform temperatures in a continuous kiln than a periodic kiln, since there are fewer heat sinks and the products are all heated in the same way. By their nature, continuous kilns are more easily loaded and unloaded than a periodic kiln. Periodic kilns are best for inconsistent or low volume production. They are very flexible, because a different curve can be run in a periodic kiln every time it is started. With a periodic kiln, two or more completely different products in one kiln can be produced without having non-productive kiln time.

There are many different kiln types; however, four basic types that are widely used in industry will be explained here. The first is the downdraft kiln which

consists of a rectangular space with a barrel-arch roof and a slotted or perforated floor which leads to flues below. Green bricks (40-100,000 at a time) are stacked in the kiln; fires are lit in fireboxes along the sides, and the hot gases pass up to the curved roof, down through the bricks and thence to the chimney stack. Wood is still used in some country areas, but most are coal, gas or oil-fired. When the desired temperature has been reached the fires are allowed to die, the kiln cools and the fired bricks are replaced by another batch of green bricks

The Hoffman kiln is the second one and the firing is continuous in it. Each day, green bricks are placed in front of the fire and fired bricks are removed from behind it, two or three adjacent areas being kept open for this purpose. When the chamber is full the areas are bricked up and fuel (coal, oil or gas) is fed in amongst the bricks through holes in the crown of the kiln. The fire is made to move forward by "taking on" a row of fire holes at the front and "dropping" a row at the back every 2-4 hours in an average size kiln. In this way the fire moves right round the kiln every 10-14 days.

The tunnel kiln, the third one, is also a continuous kiln but in this case the fire is stationary, while the bricks move through it on cars. As in the Hoffman kiln, the unfired bricks are preheated by the spent combustion gases, and air which has been heated against the cooling bricks may be drawn off to use in the associated dryers. Because of this heat interchange the tunnel kiln uses less fuel than the intermittent type of downdraft kiln, but is not as thermally efficient as the Hoffman kiln. It has several other advantages, however, principally the cars can be loaded and unloaded in the open factory, and always at the same loading points, so that handling problems are simplified and the kiln acts as a conveyor belt at the same time as it fires the bricks. Tunnel kilns vary between side-fired and top-fired kilns, the latter producing a greater degree of temperature uniformity throughout the kiln.

Lastly, Vertical Shaft Brick Kiln (VSBK) will be explained as the fourth one. It consists of one or more shafts located inside a rectangular brick structure. During operation, one batch of dried green bricks is loaded at the top at a time. A weighed quantity of powdered coal (less than 6 mm) is spread on each layer uniformly to fill the gaps. The brick unloading is done from the bottom using a trolley which runs on rails along the length of the unloading tunnel. Lifting and lowering of the trolley is done using single screw unloading mechanism. The skill in operation is to keep the firing zone in the middle of the shaft. The draught of air moving up from the bottom

cools the fired bricks in the cooling zone and it gets heated. Maximum temperature of up to 1000^{o} C is attained in the central firing zone. This recovery of sensible heat accounts for the high-energy efficiency of the VSBK technology.

PART III

TUNNEL KILN

Tunnel kilns are widely used in industry for ceramic and brick making processes. In tunnel kilns, the bricks are exposed to a series of heat treatment cycles on cars moving slowly through various temperature zones such as preheating, firing and cooling, Fig. III.1. The bricks leaving the drying kiln with a moisture content of around 12% enter the preheating zone where they encounter the hot exhaust gases from the downstream firing zone. In the preheating zone, bricks are gradually heated to evaporate the remaining water and to avoid cracking due to thermal shock. Following the preheating to 700°C, they pass to the firing zone where the pulverized coal or natural gas is fed through the holes on top of the kiln to increase the temperature up to 980°C. During the firing period, the combustion of the admixed coal, sintering reactions and crystal growth activate the formation of solid lattice within the brick body. Finally, bricks coming from the firing zone at about 980°C are cooled down to around 40°C by air flowing with varying flow rates due to suction of the hot kiln air and blowing of the ambient air into the kiln.

Modeling, optimization and control of the tunnel kilns attracted the interest of researchers as the production of bricks and ceramics in tunnel kilns is an energy intensive process. The complexity of the fluid flow, heat and mass transfer phenomena, variation of process constraints make it challenging to continue the researches to improve the operation of tunnel kiln processes.

The cooling rate of bricks is activated by the temperature difference between the bricks and air in addition to the air flow rate. Thus, blowing of the ambient air into the kiln at different locations along the cooling zone increases the temperature difference between bricks and air. Using higher flow rates to cool the bricks rapidly

increases the pressure drop. So suction of the hot kiln air is necessary to reduce the pressure drop and also to recover the heat content of the bricks. Heat recovery is required for the drying kiln where the green bricks are dried to a moisture content of about 12 %. In addition to this, some of the hot air flows from the cooling to firing zone. In the cooling zone, the bricks are cooled down to their desired final temperature of 40-60°C.

Brick arrangement in the tunnel kiln is the key point for kiln productivity, convection heat transfer between air and bricks and the specific energy consumption eduction. Furthermore, the setting characteristic such as spacing between brick loads directly effects the flow distribution along the kiln. This will also allow air circulation in the kiln and thus a uniform heating. Whatever the kiln dimensions are, the tunnel kiln operating conditions must satisfy efficient use of energy and continuous brick production.

III.1 PREHEATING

The thermal efficiency of a tunnel kiln heating system can be improved significantly by using heat contained in furnace flue gases to preheat the brick load. Therefore, when bricks enter the preheating zone, they encounter the hot exhaust gases from the firing zone that flows in the opposite direction activating the heat and mass transfers between bricks and air as shown in Fig.III.1. If exhaust gases leaving the firing zone can be brought into contact with a relatively cool incoming brick load, heat will be transferred directly to the load.

Bricks coming from drying kiln with 5-12 % moisture content on dry basis are gradually heated from about 20^{o}C to 700^{o}C to evaporate the remaining water and to avoid cracking due to thermal shock. To avoid the thermal shock due to the sudden contact of bricks with air coming from the firing zone, ambient air is supplied from the top of the kiln at several locations along the preheating zone. The air leaving the preheating zone at about between 180-200^{o}C is sucked by fans to be sent to the stack. In the stack, air contains the flue gases from the firing zone and some water vapor due to evaporation of the bound water. The amount of water vapor increases when using Natural Gas (NG) in the firing zone.

III.2 FIRING

Firing process is more complex than the processes of cooling and preheating due to the coal combustion reactions, in addition to the heat and mass transfers. These reactions are evaluated into two parts: the first deals with the combustion of admixed coal particles with the diffused oxygen into the bricks, the second discusses the reaction of the pulverized coal introduced at the top of kiln with the oxygen of fresh air as depicted in the Fig. III.1.

During the firing period, the combustion of the admixed coal, sintering reactions and crystal growth activate the formation of solid lattice within the brick. The hot air coming from the cooling zone is not sufficient to reach high temperatures for combustion of admixed coal particles and to activate strength development due to the bonding of clay particles. Therefore, the pulverized coal or natural gas and combustion air are fed through the holes from top of the kiln. The temperature of bricks increases gradually to about 980°C by the combustion of the admixed coal within the bricks and pulverized coal.

III.3 COOLING

The final step in the brick making process is to reach the desired temperature for the final product. Movement of brick loads and air in opposite directions along the kiln satisfies efficient cooling and shortens the cooling length as the temperature of the brick loads decreases.

The only and main physical mechanism taking place in the cooling zone is the heat transfer between the bricks and air. This makes mass and energy balance calculations easy for the cooling zone. Because of this simplicity, the tunnel kiln operation and optimization will be explained starting from the cooling zone. The hot bricks give off some of heat to the cooling air while moving along the cooling zone so that the bricks cool down to the desired exit temperature. In addition to the cooling air drawn from the exit of the tunnel kiln, air circulation in the cooling zone is achieved by sucking of the hot kiln air to the drying kiln and blowing of the ambient air into the kiln at different locations along the zone. The purpose is to recover the heat content of the bricks by suction of the air from the kiln and to increase the heat transfer rate between the bricks and air by blowing ambient air into

the kiln. In the cooling zone, the temperature of the bricks is reduced from about 980^{o}C to 40^{o}C.

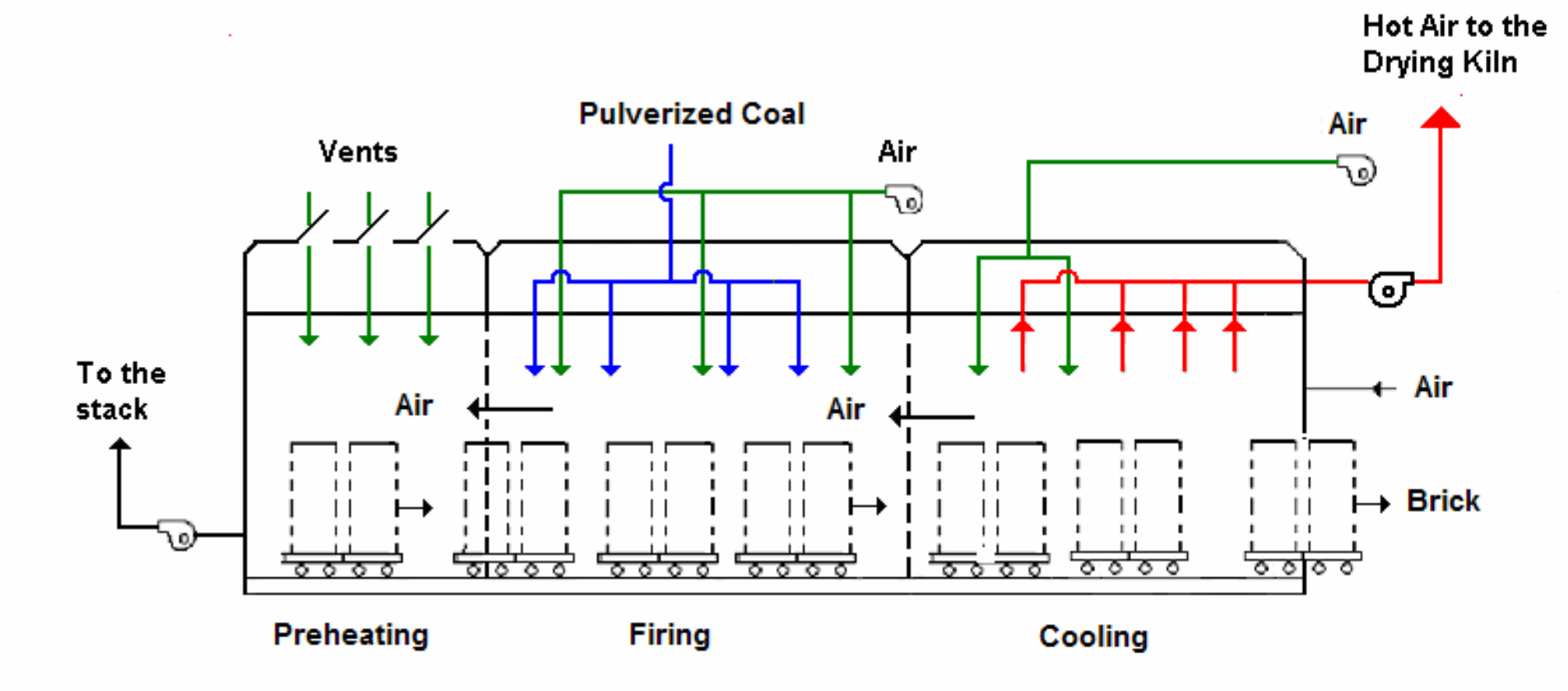

Figure III.1 Stages of Brick Making Process.

PART IV

LITERATURE SURVEY

The energy consumption in the tunnel kiln brickmaking process using different fuels for different air fuel ratios was investigated to predict the energy consumption per unit mass of brick production, Prasertsan et al. (1997), Junge (2002), Mançuhan and Küçükada (2006). The energy requirement of a tunnel kiln is a function of the type of the fuel used and the design of the kiln in addition to the brick properties. The results giving the energy requirement were reported to be varying around 2300 kJ/kg brick for different types of fuel and different air-fuel ratios (Prasertsan et al. 1997). For continuous brick production in a tunnel kiln using admixed coal, pulverized coal or natural gas, the optimum energy requirement was reported to be between 2040 and 3510 kJ/kg brick depending on the properties of fuels used (Mançuhan and Küçükada 2006). Depending on the brick type the average energy demand was estimated to be varying between 1741 and 2289 kJ/kg brick (Junge 2002).

IV.1 MODELING AND OPTIMIZATION OF TUNNEL KILN FURNACES

Mathematical models of processes are used to study the effect of operating conditions and design parameters. They can also be used to investigate the optimum operating conditions in order to minimize or maximize the objective function of the process in question in order to find optimum operating conditions. Mathematical modeling of tunnel kiln brick involves the appropriate representation of the heat transfer phenomena, air flow and combustion of the fuels used.

The first paper in this category belongs to Halasz et al. (1987) to develop an integral model for 1-D distributed-parameter tunnel kiln for minimizing the specific energy with respect to a unit product mass in the steady state of the kiln. They assumed that there is no capital for kiln redesign because of the fixed tunnel, tunnel cars and burners' construction so that calculation and setting new operational parameters can be chosen to reduce the specific energy requirement of heat treatment. As a result of this developed model 5-8 % of the used energy has been saved.

Dugwell and Oakley (1998) developed a mathematical model to predict gas temperature and composition for firing refractory ware in gas fired tunnel kilns. The prediction of the gas temperature and composition profile along the kiln and ware temperature at each point in the blade was the objective of this study. The described model was solved by integration against the gas flow, with iteration on the initial estimate of the exhaust gas temperature until correct inlet air temperature was predicted

Prasertan et al. (1997) and Caputo and Palaggage (1999) studied on modeling of continuous processes. In the former study, a computer simulation of fixed bed model for efficient energy usage in brick and design of a downdraft brick kiln were developed. The drying, preheating, firing and cooling of bricks were evaluated simultaneously by considering heat and/or mass balance. From the standpoint of energy saving, waste heat recovered from firing process was applied to the other downstream processes. The cooling zone of a moving grate kiln furnace used for iron ore sintering is simulated in the latter one. The modeling of the real time behavior of the cooling bed was based on the two dimensional schematization and on time dependent convective-conductive heat transfer.

Hilmer et al. (1998) investigated the numeric solution and validation of the dynamic behavior of solar collectors working with varying fluid flow rate for several model approximations. The dynamic behavior of the collector with a characteristic of 2-node distributed character was compared to that of several model approximations by evaluating the outlet fluid temperature.

The study of Wozny and Li (2000) can be classified in the same category from the dynamic optimization point of view. They developed methods, available tools for the planning and dynamic optimization of chemical processes. Moreover,

problem formulation, solution approaches, and practical applications were presented based on the dynamic process optimization.

Aziz and Mujtaba (2001) used the dynamic optimization techniques in order to formulate and solve maximum conversion and minimum time problems for optimal operation policies in batch reactors. The reactor temperature or coolant flow rates were the optimization variables to maximize the conversion of desired product and minimize the batch time.

The second paper of Caputo and Pelagagge (2001) in this category was based on the moving cooling bed design optimization by dealing with capital investment (bed structure, trolleys and fans) and operating expenses (blowers' operation and trolleys motion). The goal of this study was to minimize the total cost in moving cooling bed of an iron ore sintering plant. First of all, a cost function assuming the plant total annual cost as the objective function was defined. Then, heat exchange simulation model was employed in conjunction with a minimization algorithm to define the optimal bed dimensions and operating parameters. Finally, results were presented in comparison with the considered case data and by analyzing the effects of operating and economic parameters on design arrangements.

Lastly, Michael and Manesis (2005) worked on developing control methods for adjusting the required temperature profiles in tunnel kilns. In industry, the subsystems in a tunnel-type furnace are generally controlled by independent controllers. In this paper, the overall furnace system was considered from mathematical modeling and fuzzy logic based techniques points of view so it satisfies a control scheme for model based coordination of the individual subsystems. The introduced fuzzy supervisory control scheme controls local controllers and evaluates their performance criteria. Tunnel-type furnaces, because of its dynamic behavior, are complex systems so that conventional methods can fail to provide satisfactory results. Therefore fuzzy logic based techniques are important alternatives to get more accurate results for these systems.

IV.2 HEAT TRANSFER PHENOMENA

The first publication written by Theppaya et al. (1998) deals with the efficient use of energy in brick kiln divided into four separated main parts as firing, preheating, drying and cooling. This efficient use of energy was ensured by heating

up the combustion air in the cooling zone and using the exhaust gas for preheating and drying processes. According to the this paper, when the economical point of brick making process is considered, transformation of waste heat from one process to the others lowers energy usage considerably.

The study of Abdelghani-Idrissi et al. (2001) is the other one including the spatial variation of transient response of temperature for changing mass flow rate along a tubular counter flow heat exchanger. In this paper, quasi-linear first order hyperbolic PDE's in one spatial dimension were investigated in order to describe the majority of convective transfer processes. Therefore, partial states, which are the state in a suite of vectors, were distributed and estimated separately by using the numerical PDE method. That method was also applied to estimate the two fluids and the wall temperatures along a counter current heat exchanger. Finally, the estimated temperature and the experimental date were compared and if necessary, validation is done on the process.

Lastly, Abou-Ziyan (2004) investigated the effect of different brick arrangements on local and average convective heat transfer with constant heat flux. In this paper, in order to measure the local convective heat transfer coefficient from bricks, six different settings were examined for different Reynolds numbers (from 6000 to 33000) with a constant heat flux. Hence, effects of setting characteristics such as spacing between columns and bricks and effects of wall and roof gap between roof and bricks were investigated for different Reynolds number as well. The measurement was carried out with bricks in the longitudinal direction of flow and transverse to it. Furthermore, local and average convection heat transfer coefficients and pressure drop across the settings were found.

IV.3 COMBUSTION OF PULVERIZED AND ADMIXED COAL

The first paper written by Essenhigh and Mesher (1997) was based on the influence of pressure on the oxygen-carbon reaction. The prediction of reaction rates of char particles at different pressures and comparison of the predictions with experimental data taken by the study of Monson et al. that are measured at four different pressures were done. Also, the individual contributions of different factors identified such as the joint behavior of boundary layer diffusion, oxygen

chemisorption and adsorbed-film decomposition and the influence of pressure on their relative importance were shown in this study.

Förtsch et al. (2001) studied on the mass transfer coefficient for the combustion of pulverized coal particles. The effect of the boundary layer diffusional resistance for the combustion of pulverized char particles were evaluated by considering the overall reaction rate. This was done by deriving an analytical expression from the Maxwell-Stefan equations for the mass transfer coefficient for oxygen reacting with a small carbon particle in an atmosphere of O_2, N_2, CO_2, CO, and H_2O. At the end of calculations, a correction factor to the baseline case of oxygen diffusing in a stagnant gas film was obtained.

The fundamental and industrial application aspects of combustion of natural gas, heavy and light fuel oils, and coal in highly preheated air were examined by Weber et al. (2005). The scope of this study was to obtain an efficient and environment friendly combustion of various fuels from an experimental point. Thus, heat recovery methods and NO_x reduction methodologies were taken into consideration when combustion air with temperatures in excess of 1000°C was used.

Punbusayakul et al. (2006) focused on mathematical representation of the sulfation process by including the effects of temperature on the reaction rate at zero sulfation and during increased sulfate loading or accumulation of product layers. The model is relatively simple and is applicable over a wide range of temperatures, particle sizes and SO_2 concentrations. Validation was performed and it was found that the model satisfactorily represents the amount of accumulated sulfate within the entire domain of calculation.

PART V

MODELLING AND OPTIMIZATION

In attempting to develop an accurate model of the tunnel kiln, the model equations should be developed by appropriate selection of simplifying assumptions. A satisfactory model to give a sound estimation of a process should incorporate the main phenomena defined by equations in their simplest forms. A number of simplifying assumptions have been adopted in the current approach for both cooling and firing zones.

- Steady state operation, continuous travel of brick packages.
- Counter current flow of air and bricks. The variation of the temperatures and air flow rates in the vertical direction was not taken into account.
- Heat is transferred between the cooling air and bricks predominantly by convection.
- Concerning the radiative heat transfer, the kiln walls and the exterior surfaces of the brick loads were considered being the two surfaces seeing each other.
- Heat content of kiln cars is very close to the heat content of the brick loads. Therefore, the kiln cars were considered as brick loads while solving the model equation.
- The kiln roof is made up of two separate walls, Fig. V.3, between which the roof cooling air flows. The purpose of roof cooling air is to avoid the heat loss from the roof. The hot roof cooling air is sent to the stack to avoid the risk of condensation. It does not intervene with the air flowing through the brick loads.
- Heat loss from the kiln walls was neglected.

The following assumptions are used to develop the necessary model equations for the firing zone:

- Carbon equivalent values were used for combustion of both pulverized and admixed coals.
- Pulverized coal reacts with oxygen instantaneously.
- Using the heating values of the admixed coal (AC) and pulverized coal (PC), the equivalent carbon was calculated and it was used in calculating the carbon reaction rate.
- Combustion of admixed coal takes place within the bricks and is controlled by the diffusion of oxygen and reaction kinetics.
- In the firing zone, combustion of pulverized coal fed from the top of the kiln was considered to be spontaneous. In other words it was considered as a heat source.

V.1 MODELING OF HEAT TRANSFER PHENOMENA

In the tunnel kiln, there are two differences between the cooling and firing zones. The first difference is the temperature difference between the bricks and air. The second difference is the removal of the hot kiln air in the cooling zone. The combustion of the admixed and pulverized coal defines the temperature profile along the firing zone whereas the periodic suction of the hot kiln air and blowing of the cold ambient air define the temperature profile in the cooling zone. In the firing zone the bricks enter at a temperature lower than the air temperature. The combustion of the admixed coal starts and bricks reach temperatures higher than the air temperature. However in the cooling zones bricks temperature is always higher than the air temperature and heat is transferred by convection from bricks to air.

V.1.1 Heat Transfer Phenomena in the Cooling Zone

Heat is transferred between the cooling air and bricks by convection. The hot bricks from firing zone give off some of heat to the cooling air while moving along the cooling zone so that bricks cool down to the desired exit temperature. Temperature difference between the bricks and air is the driving force for heat transfer. Thus the larger the temperature difference between the brick and air, the

higher the rate of heat transfer. In the real plant, the temperature difference is increased at two different locations by blowing a certain amount of ambient air into the kiln, Fig. V.1. In addition, radiative heat transfer becomes significant at the region close to the brick inlet side of the cooling zone. The heat transferred by radiation occurs between the exterior surfaces of the brick loads and the interior walls of the kiln.

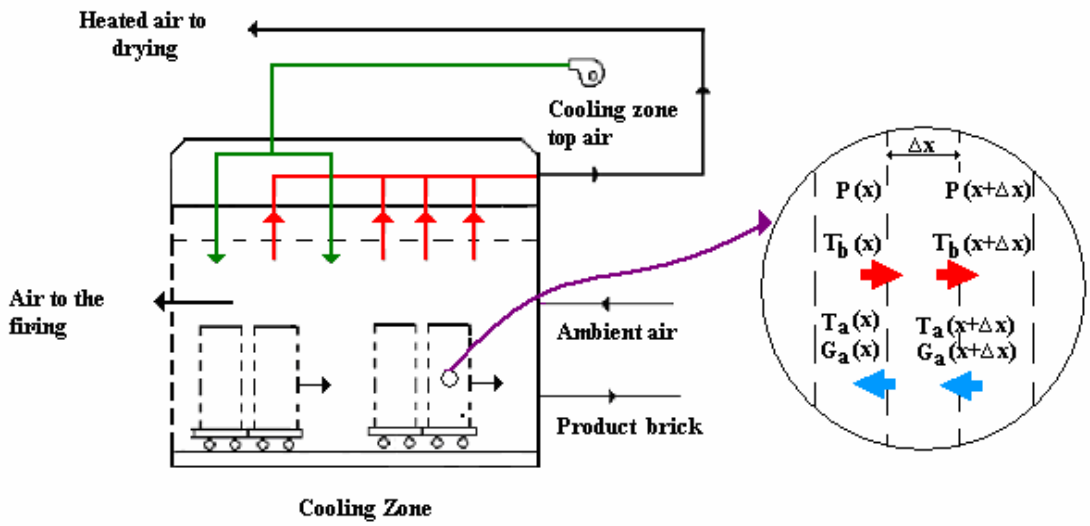

Figure V.1. Cooling Zone of the Tunnel Kiln

Model equations were derived for a differential length increment, Δx, along the cooling zone of the tunnel kiln as shown in figures V.1 and V.2. Superficial mass flow rate of air for each Δx length interval enables us to investigate the trend of air flow rate, temperature profiles and pressure drop along the cooling zone.

The ambient air flow rate at the brick exit side, $G_a(\bar{L})$, suction or blowing air flow rates, $g_a(x)$, are the optimization variables for the cooling zone. Both determine the profile of the superficial air mass flow rate, $G_a(x)$, within the cooling zone. This in turn controls the pressure drop and heat transfer rate in the cooling zone. In Eq. (V.1), $g_a(x)$ represents the mass flow rate of either the suction or blowing air in the cooling zone.

$$G_a(x) = G_a(x+\Delta x) + g_a(x) \qquad \text{(V.1)}$$

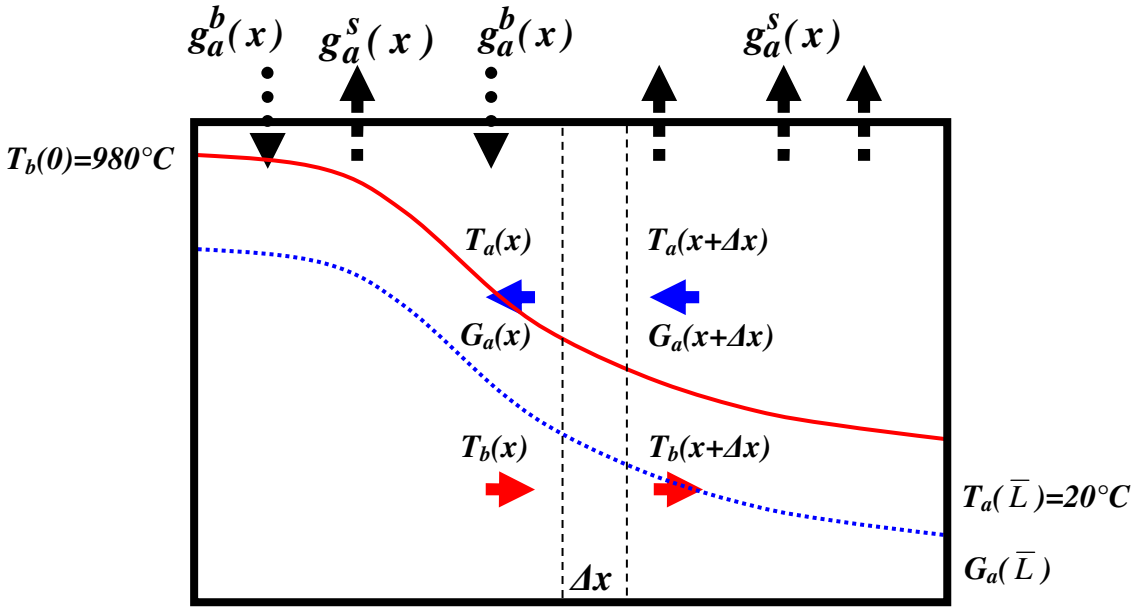

Figure V.2 Differential Length Element and State Variables Used to Derive the Model Equations

The flow of air and bricks is countercurrent. The temperature of the air increases as it flows from the cooling zone exit side to the entrance side. The differential energy balance between the bricks and air can be written as follows:

$$\left\{\begin{array}{c}\text{Heat gaine d by air}\\ \text{along the different ial}\\ \text{length } \Delta x\end{array}\right\}=\left\{\begin{array}{c}\text{Heat trans ferred}\\ \text{by convect ion}\\ \text{between the brick s and air}\end{array}\right\} \qquad \text{(V.2)}$$
$$+\left\{\begin{array}{c}\text{Heat trans ferred}\\ \text{by convect ion betwee n}\\ \text{the air an d ki ln walls}\end{array}\right\}+\left\{\begin{array}{c}\text{Heat sin k}\\ \text{or source term}\end{array}\right\}$$

The above described energy balance can be written in differential form as follows:

$$\frac{d[G_a C_{pa} T_a]}{dx}=h_b a_b[T_b-T_a]+h_w a_w[T_w-T_a]+q_a^{s,b}(x) \qquad \text{(V.3)}$$

The last term to the right of Eq. (V.3), $q_a^{s,b}(x)$, acts as a sink or source term due to suction or blowing. At suctions, dG_a/dx will be smaller than zero and thus energy leaving the differential length element, $T_a\ C_{pa}\ dG_a/dx$ will have negative sign. On the other hand, when the ambient air is introduced into the cooling zone, dG_a/dx, is greater than zero and thus the energy supplied by the ambient air is $C_{pa}\times(20°C)\times dG_a/dx$.

Heat transferred by convection to the air together with the heat transferred to the kiln interior walls by radiation is equal to the heat lost by bricks along Δx, and can de described by the following equation:

$$\left\{\begin{array}{c}\textit{Heat lost by bricks}\\ \textit{along the differenti al}\\ \textit{length } \Delta x\end{array}\right\}=\left\{\begin{array}{c}\textit{Heat transferre d}\\ \textit{by convection}\\ \textit{between the bricks and air}\end{array}\right\}+\left\{\begin{array}{c}\textit{Heat transferre d}\\ \textit{to the kiln interior walls}\\ \textit{by radiation}\end{array}\right\} \tag{V.4}$$

The differential heat balance for bricks can be given by the following equation, Eq. (V.5).

$$-G_b C_b \frac{dT_b}{dx} = h_b\, a_b \left[T_b - T_a\right] + F_{bw}\, \sigma\, \varepsilon\, a_w \left[T_b^4 - T_w^4\right] \tag{V.5}$$

In the firing and cooling zones, bricks are at a higher temperature than the kiln wall. All surfaces within industrial furnaces, emit, reflect and absorb radiation from their surroundings and thereby participate in the overall exchange of radiant energy. Heat is transferred from bricks to wall by radiation and from air to wall by convection. However there may be regions along which heat is transferred from the kiln wall to the kiln inside air by convection when the wall temperature is higher than the air temperature. By writing the heat balance equation on the wall, the wall temperature at any location along the cooling zone can be written as follows:

$$\left\{\begin{array}{c}\textit{Heat trans ferred}\\ \textit{through th e ki ln walls}\\ \textit{by conduc tion}\end{array}\right\} = \left\{\begin{array}{c}\textit{Heat trans ferred}\\ \textit{by convect ion}\\ \textit{between th e air and ki ln wall}\end{array}\right\} + \left\{\begin{array}{c}\textit{Heat trans ferred to the ki ln}\\ \textit{int erior wall s by radia tion}\\ \textit{from the brick load s}\end{array}\right\} \tag{V.6}$$

In case of neglecting the heat loss through the kiln wall, the term to the left hand side of the above equation disappears and the differential heat balance for walls can be given by the following equation, Eq. (V.7).

$$h_w a_w [T_w - T_a] = F_{bw} \sigma \varepsilon a_w \left[T_b^4 - T_w^4\right] \quad \text{(V.7)}$$

In other words, the heat transferred due to radiation between the brick loads surface and the kiln interior wall is equal to the heat transferred by convection between the kiln interior wall and air. Then Eq. (V.7) can be used to predict the kiln interior wall temperature.

The air and brick inlet temperatures are 20°C and 980°C respectively. These values are used for solving the above given model equations.

$$T_a(\bar{L}) = 20\,^oC; \quad T_b(0) = 980\,^oC \quad \text{(V.8)}$$

In the above equalities, $\bar{L}$, represents the brick exit side where most of the cooling air is introduced into the kiln due to suction. The air inlet temperature changes depending on the weather conditions, whereas an average value of 20°C was assumed for calculations.

The above equations need to be solved numerically by writing each equation N times in discretized form for each Δx length along the kiln. The equations in discretized forms are given in Appendix A.

V.1.2 Heat Transfer Phenomena in the Firing Zone

Heat transfer mechanism in the firing zone is more complex than that of the cooling zone. As soon as the pulverized coal is introduced at the top of the firing zone, they burn by reacting with the oxygen of air. Since coal combustion is an exothermic reaction, the released heat increases the air temperature in the firing zone. The heat energy is transferred by convection between the air and the brick throughout the firing zone due to the temperature difference existing between these substances, whereas the direction of heat transfer shows changes depending on the temperatures of the air and the brick at that point.

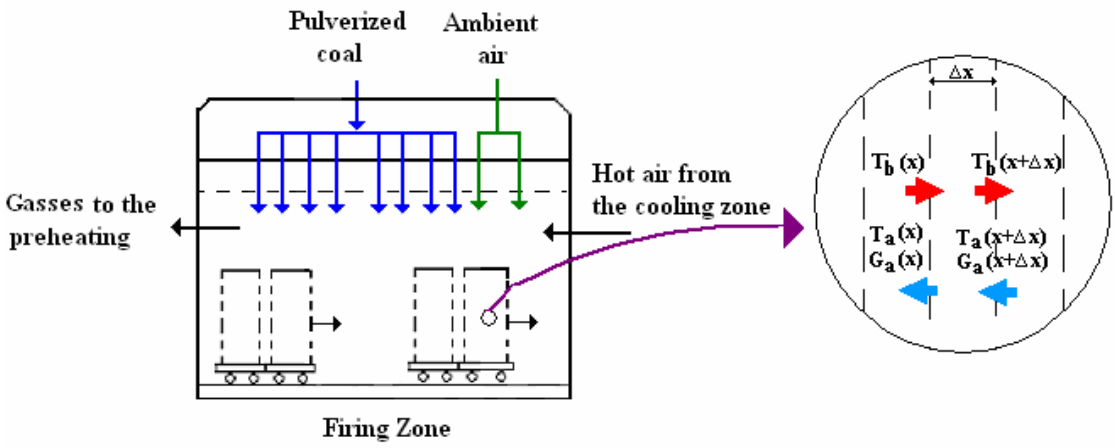

Figure V.3 Firing Zone of the Tunnel Kiln

Similar to the cooling zone model equations were derived for a differential length increment, Δx, including the heat released by combustion of the pulverized and admixed coals. The state variables used in the model equations along the firing zone were shown in figures V.3 and V.4.

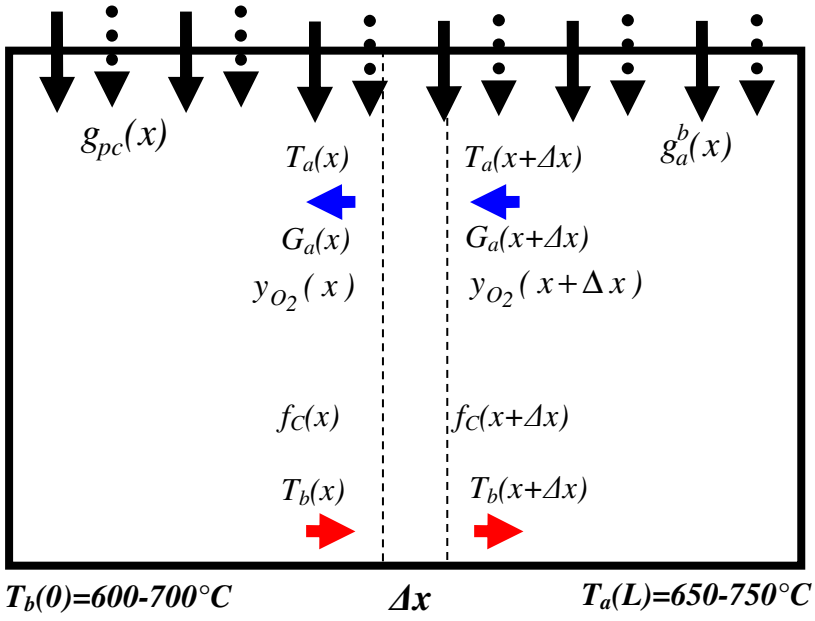

Figure V.4 Differential Length Element and State Variables Used to Derive the Model Equations

In Eq. (V.9), $g_a^b(x)$ represents the mass flow rate of the secondary air for combustion of fuels in the firing zone. The hot air flow rate coming from the cooling to the firing zone is $G_a(\overline{L})$. Both determine the profile of the superficial air mass flow rate, $G_a(x)$, within the firing zone.

$$G_a(x) = G_a(x+\Delta x) + g_a^b(x) \qquad \text{(V.9)}$$

The temperature of the air increases as it flows from the firing zone exit side to the entrance side. The differential energy balance between the bricks and air gives the following equation:

$$\left\{\begin{array}{c}\textit{Heat gained by air}\\ \textit{along the differential}\\ \textit{length } \Delta x\end{array}\right\} = \left\{\begin{array}{c}\textit{Heat transferred}\\ \textit{by convection between}\\ \textit{the bricks and air}\end{array}\right\} + \left\{\begin{array}{c}\textit{Heat transferred}\\ \textit{by convection from}\\ \textit{the air to the kiln walls}\end{array}\right\} + \left\{\begin{array}{c}\textit{Heat input}\\ \textit{by blowing of}\\ \textit{the ambient air}\end{array}\right\} + \left\{\begin{array}{c}\textit{Heat released by}\\ \textit{combustion of}\\ \textit{the pulverized coal}\end{array}\right\} \qquad \text{(V.10)}$$

The above described energy balance can be written in differential form as follows:

$$\frac{d[G_a C_{pa} T_a]}{dx} = h_b a_b [T_a - T_b] + h_w a_w [T_a - T_w] + T_0 C_{p_a} \frac{dG_a}{dx} + \frac{dg_{pc}}{dx} \Delta H_{pc} \qquad \text{(V.11)}$$

The third term to the right of the equation acts as a source term due to blowing. If the hot air is not sufficient for complete combustion of admixed and pulverized coal then blowing of the secondary air is necessary in the firing zone. Similarly, the last term to the right of the equation represents the energy released due to instantaneous combustion of the pulverized coal.

Heat transferred by convection to the air together with the heat transferred to the kiln interior walls by radiation is equal to the heat lost by bricks along Δx, and can de described by the following equation:

$$\left\{\begin{array}{c}\textit{Heat lost by bricks}\\ \textit{along the differential}\\ \textit{length } \Delta x\end{array}\right\}=\left\{\begin{array}{c}\textit{Heat transferred}\\ \textit{by convection between}\\ \textit{the bricks and air}\end{array}\right\} + \left\{\begin{array}{c}\textit{Heat transferred}\\ \textit{to the kiln interior}\\ \textit{walls by radiation}\end{array}\right\}+\left\{\begin{array}{c}\textit{Heat released}\\ \textit{by combustion of}\\ \textit{the admixed coal}\end{array}\right\} \tag{V.12}$$

The differential heat balance for bricks can be given by the following equation:

$$-G_b C_{pb}\frac{dT_b}{dx} = ha_c\left[T_a - T_b\right] + F_{bw}\sigma\varepsilon a_w\left[T_b^4 - T_w^4\right] + G_b\frac{df_C}{dx}\Delta H_{ac} \tag{V.13}$$

An inlet condition is a state restriction that is imposed on the solutions of model equations to limit the possible solutions. The air and brick temperatures are calculated for the inlet conditions as follows:

$$T_a(L) = 650 - 750^o C;\quad T_b(0) = 600 - 700^o C \tag{V.14}$$

The first condition represents the temperature of air coming from the cooling to the firing zone. Brick inlet temperature to the firing zone is the temperature reached in the preheating zone and it is around 600-700°C.

The equation giving the heat balance on the kiln interior wall, Eq. (V.7) in section V.1.1, is used to represent the heat transfer on the surface of the kiln wall. The correlations to calculate the convective heat transfer coefficient and the properties of air and brick were given in Appendix B.

V.2 AIR FLOW AND PRESSURE DROP

Pressure drop is the reduction in air pressure from one point to another due to the friction of the flowing air through the the brick holes and spacing. The spacing in question is the gaps above the brick loads and between the kiln walls and brick loads as shown in Figure V.5. The pressure drop for a differential length element was obtained using Eq. (V.15) from the Darcy-Weisbach equation where *f* is the Fanning friction factor given in Appendix C.

$$\frac{dP}{dx} = 4f\frac{\rho_a\ v_a^2}{2D_e} = 2f\frac{\rho_a}{D_e}\left(\frac{G_a}{\rho_a}\right)^2 \qquad \text{(V.15)}$$

In the above equation, the friction factor, f, density, ρ_a, and air mass flow rate, G_a, all change along the cooling zone. The correlations to calculate the friction factor as a function of the Reynolds number is given in the Appendix C. The equivalent diameter, D_e, for different brick arrangements was reported to be varying between 3.5 and 5.5 cm by Abou-Ziyan (2004). Using sizes of commonly produced bricks by the existing tunnel kiln, an average value of the hydraulic radius was calculated to be between 0.75 and 1.2 cm. By definition the equivalent diameter is four times the hydraulic radius. Then the value of D_e, is between 3.0 and 4.8 cm. In the computations an average value of 4.0 cm was used. Temperature has a major effect on the pressure drop across the bed, which, in turn, can influence the gas flow rates. An increase in air temperature will increase the air velocity if the air mass flow rate remains constant.

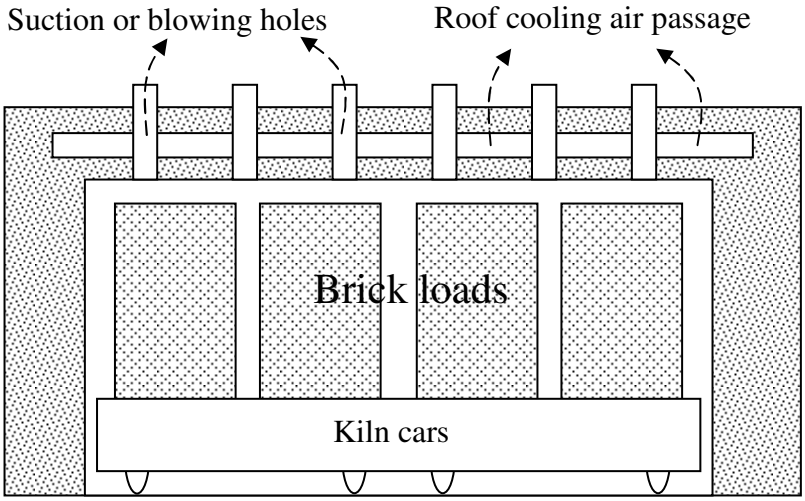

Figure V.5 Cross Section View of the Tunnel Kiln with Brick Loads and Kiln Car

V.3 COMBUSTION OF ADMIXED COAL

The temperature of bricks coming from the preheating zone is about 700°C and should increase gradually to temperatures around 1000°C due to combustion of admixed coal in the bricks and pulverized coal supplied from the top of the kiln. Before the carbon of admixed coal reacts with oxygen, the free energy of the system

must overcome the activation energy for the combustion reaction. Although hot air coming from the cooling zone provides that required energy to initiate the carbon combustion in large amounts, it is not enough. Therefore, the pulverized coal introduced at the top of the kiln is used to satisfy the remaining energy requirement. Two combustion reactions take place in the firing zone as combustion of admixed coal and combustion of pulverized coal. Combustion of admixed coal was considered taking place together with the oxygen diffusing in the bricks. For complete combustion, essential oxygen must be present in the considered medium. Hence, diffusion of oxygen in the bricks takes an important role in the combustion reaction of admixed coal. The porous structure of bricks allows oxygen to diffuse through the bricks so the carbon in the bricks reacts with the diffused oxygen by releasing carbon dioxide at high temperatures as combustion product. That released hot gas would cause an increase in the brick temperature.

The combustion of the admixed coal in the bricks was defined by the following equation and its derivation was outlined in Appendix D.

$$-G_b \frac{d f_C}{dx} = k a_{C0} f_C^{2/3} C_{O_2} \qquad \text{(V.16)}$$

The change of O_2 concentration along the length element, Δx:

$$\frac{d(G_a C_{O_2} / \rho_a)}{dx} = -\left[f_{pc} \frac{dg_{pc}}{dx} + G_b \frac{df_{ac}}{dx} \right] \frac{1}{MWc} \qquad \text{(V.17)}$$

Considering that the gas mixture as an ideal gas, the mole fraction of O_2 and CO_2 can be calculated using the following relation:

$$y_j = \frac{C_j}{P/RT}. \qquad \text{(V.18)}$$

At the end of the firing zone, the fresh air enters from the cooling zone and thus, the necessary inlet conditions to solve the above equations are:

$$y_{O_2}(\bar{L}) = 0.21 \;\; ; \;\; y_{CO_2}(\bar{L}) = 0.0 \qquad \text{(V.19)}$$

There are two other conditions to be used while solving the model equations. These are the air flow rate coming from the cooling zone and the admixed carbon fraction in the bricks. The air flow rate coming from the cooling zone, $G_a(L)$, should be computed as a result of the optimization of the cooling zone. The initial carbon content in the bricks, $f_c(0)$, is one of the optimization variables for the firing zone.

Kinetics of combustion and combustion rate of coal are strongly influenced by the properties of the coal and the combustion medium. The heat of combustion of carbon is 32 790 kJ/kg and the combustion takes place almost instantaneously at temperatures above 600°C.

$$C + O_2 \rightarrow CO_2$$

Many studies investigated the combustion kinetics of coal and other carbon containing solid fuels such as coke breeze. Combustion of coke at temperatures 800, 900 and 1070°C was investigated by Iwanaga and Takatani (1989) and a rate constant as 3.78×10^7 exp(-188 936/R T) in units of m/s was proposed stating that the combustion rate is controlled both by the diffusion of oxygen and combustion kinetics. Similarly Smith (1978) reported that the activation energy of the combustion of different carbonaceous materials vary between 126 and 290 kJ/mole depending on the coal type, temperature, particle size and oxygen pressure. The rate constant in kg/m^{2}s was given as 3050 exp(-179400/R T) and it was also reported that the reaction rate is first order with respect to the partial pressure of oxygen.

Concerning the combustion of the pulverized coal, it was assumed that as soon as the pulverized coal is introduced at the top of the firing zone, it burns immediately by reacting with the oxygen of air. Since coal combustion is an exothermic reaction, the released heat increases the air temperature in the firing zone. The heat energy is transferred by convection between the air and the brick throughout the firing zone due to the temperature difference whereas the direction of heat transfer shows changes (either from brick to air or vice versa) depending on the temperatures of the air and the brick at that point.

V.4 OPTIMIZATION

Process optimization deals with finding the optimum operating conditions in order to minimize the objective function. The process constraints define the bounds of the optimization variables. Optimization variables and constraints change with position for the considered system to satisfy the constraints. Therefore, model equations are written in discretized forms as it was given in Appendix A for each length increment, Δx, along the cooling zone as shown in Fig. V.6

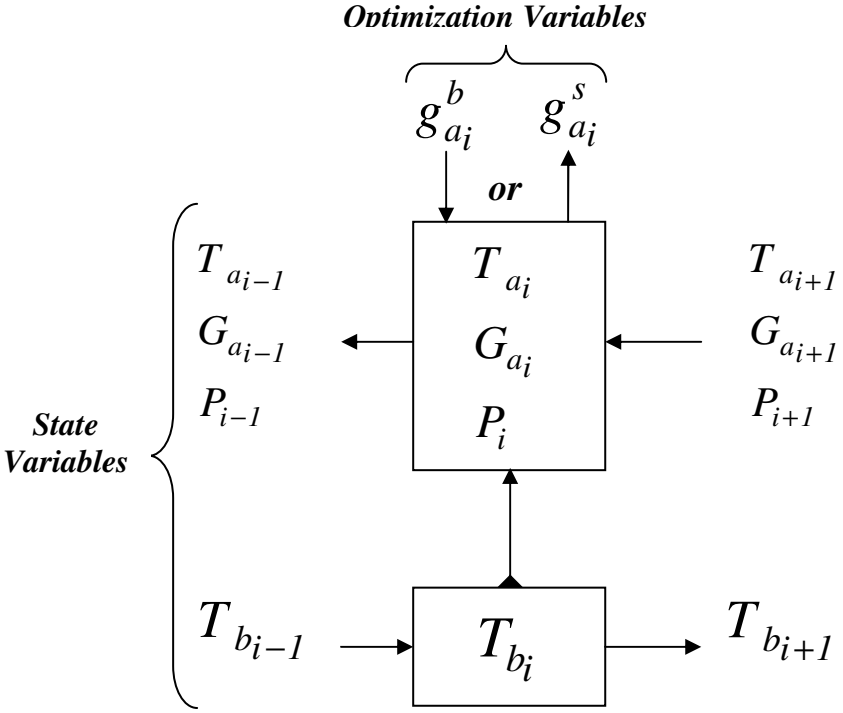

Figure V.6 Flow Diagram for the Differential Length Element along the Cooling Zone

Whatever the zone to be optimized, the approach is the same. The model equations should be solved to minimize or maximize the objective function under the constraints. The objective function for the cooling zone is the pressure drop along the cooling zone.

Similarly the optimization of the firing zone can be done by considering it as a decomposable structured system as shown in Fig. V.7. While optimizing the firing zone the objective function is the minimization of the cost of fuels used.

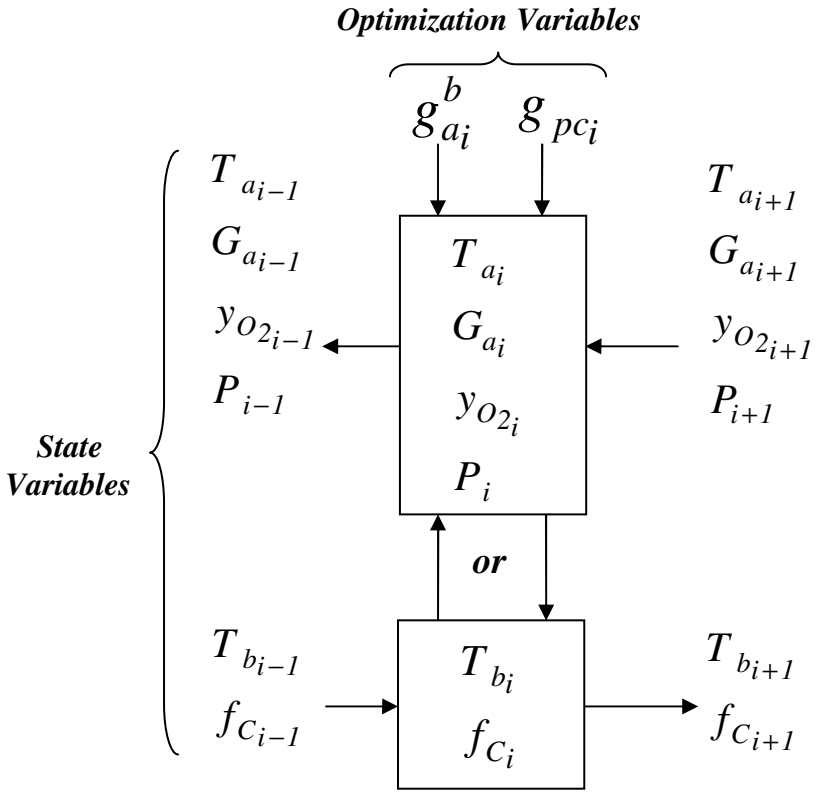

Figure V.7 Flow Diagram for the Differential Length Element along the Firing Zone

V.4.1 Optimization of the Cooling Zone

The pressure drop along the cooling zone is a function of the flow rate of the air passing through the cooling zone and temperature of the air. The fresh air entering at the cooling exit side, the suction and blowing air flow rates need to be optimized to increase the heat transfer between the bricks and air while minimizing the total pressure drop. This goal is formulated as:

$$min \sum_{i=1}^{N} \Delta P_i = min \int_0^L \frac{dP(x)}{dx} dx = min \int_0^L 2 f(x) \frac{\rho_a(x)}{D_{eq}} \left(\frac{G_a(x)}{\rho_a(x)} \right)^2 dx \qquad \text{(V.20)}$$

The optimization variables for the cooling zone are:

- The suction or blowing air flow rates, $g_a^{s,b}(x)$.
- Inlet ambient air flow rate at the cooling zone brick exit side, $G_a(\bar{L})$.

In order to minimize the objective function to predict the optimization variables, the process constraints should also be considered. The constraints to be satisfied are:

- Brick exit temperature,

$$T_b(\bar{L}) \le 40^o C$$

- Heat required in the drying kiln,

$$\sum_{i=1}^{N} (g_a^s C_{pa} T_a)_i \ge q_{dry}$$

- Maximum temperature difference between bricks and air to avoid thermal shock,

$$T_b(x) - T_a(x) \le \Delta T_{max}^{ba}$$

- Maximum cooling rate to avoid thermal shock,

$$\frac{G_b}{\rho_b}\frac{dT_b}{dx} \le \dot{\Theta}_{max}$$

Maximum temperature difference, ΔT_{max}^{ba}, to which bricks can be exposed and the maximum cooling rate, $\dot{\Theta}_{max}$, are functions of brick properties such as thickness, density, heat capacity, thermal conductivity, thermal expansion coefficient, modulus of elasticity, tensile stress and the convective heat transfer coefficient Vogt and Vogt (2004). The mechanical properties of common masonry bricks were given in Appendix B.

Model equations should be solved simultaneously to find the temperature profiles for air and bricks by using the numerical methods for a given set of suction and blowing air flow rates. The iterative computations were done until a satisfactory convergence between two successive set of temperature profiles and minimum pressure drop given by were obtained.

V.4.2 Optimization of the Firing Zone

The objective function of the firing zone is the fuels cost and it must be minimized by finding the optimal flow rate of the pulverized coal, admixed coal within the bricks in addition to flow rate of the secondary air fed from top of the kiln. The objective function for the firing zone can be written as:

$$min\{J(f_{ac0}, g_{pc}(x))\} = min\left\{J_{ac} G_b f_{ac0} + J_{pc} \sum_{i=1}^{N} g_{pc\,i}\right\} \qquad \text{(V.21)}$$

The optimization variables in the firing zone are:

- The initial admixed coal percentage in the brick body, f_{C_0} .
- The mass flow rate of the pulverized coal added at different locations from the top of the firing zone, $g_{pc}(x)$.
- Flow rate of the secondary air fed at different locations along the firing zone, $g_a^b(x)$.

The constraints to be satisfied are:

- The admixed coal within the brick body should be consumed completely at the end of the firing zone, $f_C(\overline{L}) \cong 0.0$.
- The carbon percentage in the brick body, f_{C_0} , should not exceed the permissible limit. It should be as low as 3% with a maximum permissible limit of 6%.
- Maximum temperature difference between bricks and air to avoid thermal shock,

$$T_b(x) - T_a(x) \leq \Delta T_{max}^{ba}$$

- Maximum heating rate to avoid thermal shock,

$$\frac{G_b}{\rho_b}\frac{dT_b}{dx} \leq \dot{\omega}_{max}$$

- The admixed coal is a low grade coal with a carbon percentage of around 20%.

The secondary air fed into the firing zone is required for complete combustion of both admixed and pulverized coal. However, it should be kept as minimum as possible since the secondary air will have a cooling effect in the firing zone. Practically there may not be any requirement for the secondary air if the hot air coming from the cooling zone is sufficient for complete combustion.

In the present tunnel kiln investigated, a kiln car of a length of 4 m is pushed into the kiln every 20 minutes. This gives an average kiln car speed of 10 m/h. The hot air coming from the cooling zone supplies some of the energy required to heat up the bricks to elevated temperatures. In addition, it supplies the oxygen required for combustion of admixed and pulverized coal. Its value is predicted after the optimization of the cooling zone. Increasing the temperature of the hot air from the

cooling zone will slow the cooling process. On the other hand, increasing its flow rate will increase the pressure drop.

Because of the discontinuity due to suction and blowing air flow rates, and feed of the pulverized coal model equations cannot be solved analytically. Writing the model equations in discretized form helps us to define the process as a stage-wise decomposable structured system. Optimization methods for the decomposable structured systems and trajectory optimization of lumped parameter systems were explained in detail by Ray and Szekely (1973). Solver option of Excel is used to solve the model equations in order minimize the objective function under the given constraints.

PART VI

RESULTS AND DISCUSSION

The results obtained using the model, were compared to the industrial data gathered from an existing kiln. The overall mass and energy balances were computed for cooling and firing zones and these results were presented in section VI.1. First the results for the cooling zone will be presented because of its simplicity. Following the analysis of the cooling and firing zone data in section VI.1, the optimized results will be presented for the cooling and firing zones in section VI.2. In sections VI.1 and VI.2, the computations were done for 1 kg/m^{2}s brick flow rate. The measured mass flow rates of air, brick and fuel were divided by the mass flow rate of the bricks produced. This step is used to define dimensionless flow rates per kg of brick produced. In the model equations the flow rates were multiplied by 1 kg/m^{2}s brick flow rate to convert the dimensionless flow rates of air and fuel to superficial mass flow rates of air and brick.

VI.1 DATA OBTAINED FROM THE EXISTING TUNNEL KILN

The plant data have been collected from an existing tunnel kiln of a brick company. The following parameters were monitored for this aim:

- Physical dimensions of tunnel kiln, physical dimensions and properties of brick loads, load rate of kiln cars, the location of suction and blowing holes, the location of pulverized coal and secondary air holes,
- Pulverized coal and secondary air mass flow rates,
- Initial fraction of the admixed coal within the brick body,

- The suction and blowing air mass flow rates in the cooling zone,
- Temperature and pressure measurements along the tunnel kiln.

VI.1.1 Cooling Zone Data

In the existing tunnel kiln, there are total four suction and two blowing locations along the cooling zone (Fig. VI.1). The three suction sets are consecutive starting from the cooling exit.

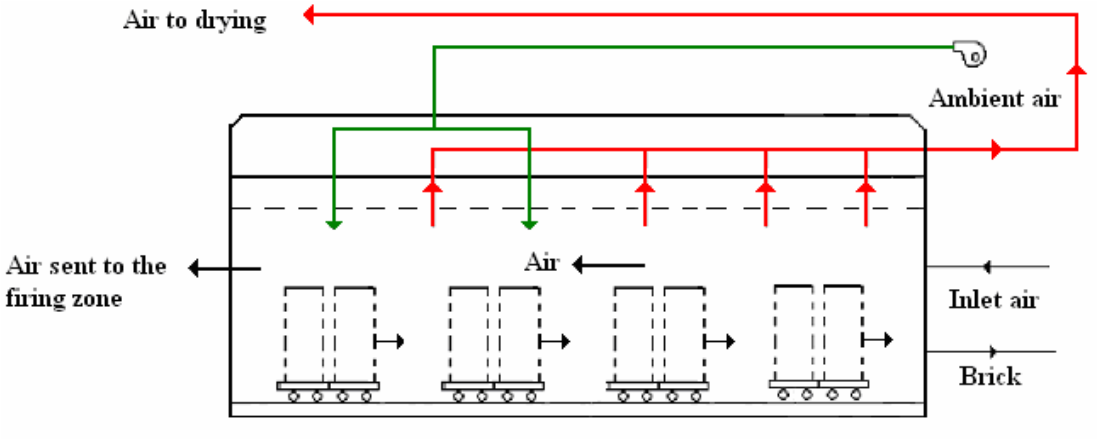

Figure VI.1 Schematic Representation of the Cooling Zone

The amounts of air sucked were assumed to be distributed equally from four set of holes, Table VI.1. Similarly, the ambient air was blown into the kiln through the two set of holes. In the cooling zone of the existing tunnel kiln, the air flow rate varies periodically and decreases from 5.76 to 0.8 kg/m^2 s by regular suction and blowing of the air at different locations, Table VI.1. At the location where the fourth and last set of suction holes (close to the beginning of the cooling of bricks), the air flow rate reaches to its minimum value at 0.32 kg/m^2 s.

Table VI.1 Suction and Blowing Air Flow Rates, Superficial Air Flow Rate, Measured Temperatures along the Cooling Zone of the Existing Tunnel Kiln

	Brick inlet	Blowing 2	Suction 4	Blowing 1	Suction 3	Suction 2	Suction 1	Brick exit
$\overline{L}$ (%)	0	6	16	25	31	53	78	100
$g_a^{s,b}$ (kg/m^{2}s)	NA	0.48	-1.48	0.48	-1.48	-1.48	-1.48	NA
G_a (kg/m^{2}s)	0.8	0.8	0.32	1.80	1.32	2.80	4.28	5.76
T_m (°C)	814			602		402	220	40

The overall mass and energy balances were computed around the cooling zone by using data collected from the industrial plant and the results were given in Table VI.2. At the entrance of the cooling zone, kiln cars have a heat content of 887.4 kJ/kg brick while the brick loads have 819.3 kJ/kg brick. So in the solution of the model equations kiln cars can be considered as brick loads. In order to compensate the heat load of the kiln cars, the computations were done for a brick flow rate of 2.083 kg/m^2 s as basis. The temperature of air sucked from the cooling zone was measured to be between 188 and 200°C in Table VI.2. Hot air temperature from cooling to firing zone was calculated to be 800°C by computing mass and energy balances around the cooling zone for the existing tunnel kiln.

Table VI.2 Mass and Energy Balances around the Cooling Zone for Existing Tunnel Kiln

	Mass flow rate ratio (kg/kg brick)		Temperatures (^oC)		Heat flow rate ratio (kJ/kg brick)	
	In	Out	In	Out	In	Out
Inlet air from the tunnel kiln exit	5.76		20		115.6	
Air blown for cooling	0.96		20		19.3	
Air sucked for drying kiln		5.92		192.3		1142.1
Hot air from cooling to firing		0.8		800		642.0
Bricks	1	1	980	33	819.3	27.6
Kiln cars	1.083	1.083	980	33	887.4	29.9
Total Balance	8.803	8.803			1841.6	1841.6

In Table VI.1, the measured temperature was given as 814°C at the entrance of the cooling zone. This is a value between the temperature of bricks, 980°C, and of air. The energy exchange around the system boundaries was calculated as 1841.6 kJ/kg brick after the mass and energy balance computations around the cooling zone.

VI.1.2 Firing Zone Data

The temperature of bricks coming from the preheating zone is about 600^{o}C and increases gradually to about 980^{o}C due to combustion of admixed coal in the bricks and pulverized coal fed through the holes on top of the kiln. Firing zone requires the use of air as heat transfer medium and for complete combustion of the fuels used. Air is supplied from the brick exit side of the firing zone and also as

secondary air from the top of the kiln. Theoretically the inlet and outlet temperatures of the air should be the same for an efficient use of the energy supplied by fuels.

Based on a very simple calculation, the energy requirement to increase the temperature of bricks from 600 to 1000 is at least 334.6 kJ/kg brick neglecting the heat loss. The heat required by kiln cars is 1.083×334.6=362.4 kJ/kg brick. Then the total energy required in the firing zone neglecting the energy required by air is 697.0 kJ/kg brick (334.6+362.4). Any decrease in the temperature of air coming from the cooling zone will increase the fuel required in the firing zone. For example if the temperature of air rises from 600 to 700°C, then the amount of energy required by air becomes 113.0 kJ/kg air. If the ratio of the air to brick mass flow rates is 1 kg air/kg brick then the total energy requirement in the firing zone may be at least 810 kJ/kg brick (697.0+113.0).The heating value of the admixed and pulverized coal samples were measured in the laboratory using the bomb calorimeter and the results were given in Table VI.3. The heating value of the admixed coal shows significant variations since the samples of admixed coal contain sand and clay which makes it suitable to be used in the brick body as a raw material as well as heat source.

Table VI.3 Measured Heating Values of Admixed and Pulverized Coals

	Heating Value (kJ/kg)	
	Admixed Coal	**Pulverized Coal**
1	2244,66	15265,36
2	2317,81	19069,16
3	2317,81	18776,56
4	3122,46	18191,36
5	3780,80	16362,61
6	4439,16	15411,66
7	4585,46	16874,70
8	6926,30	16289,50
9	6999,42	16216,31
10	8681,90	16289,46
Mean	4541,58	16874,67
St. dev.	2276.48	1344.84

Using the mean heating values it can be calculated that the heat requirement of 810 kJ/kg brick can be supplied either by using 0.178 kg admixed coal

(810/4541.58) or 0.048 kg pulverized coal (810/16874.67) per kg of brick produced. The admixed coal may contain approximately 20% of carbon which creates pores within the bricks. The permissible limit of carbon percentage within the bricks is 3% with a tolerance of up to 6%. If the admixed coal is 0.178 kg admixed coal per kg of brick then the carbon percentage within the bricks will be 3.56% which is greater than the permissible limit. This calculation shows simply the use of constraints on finding the amounts of admixed and pulverized coals.

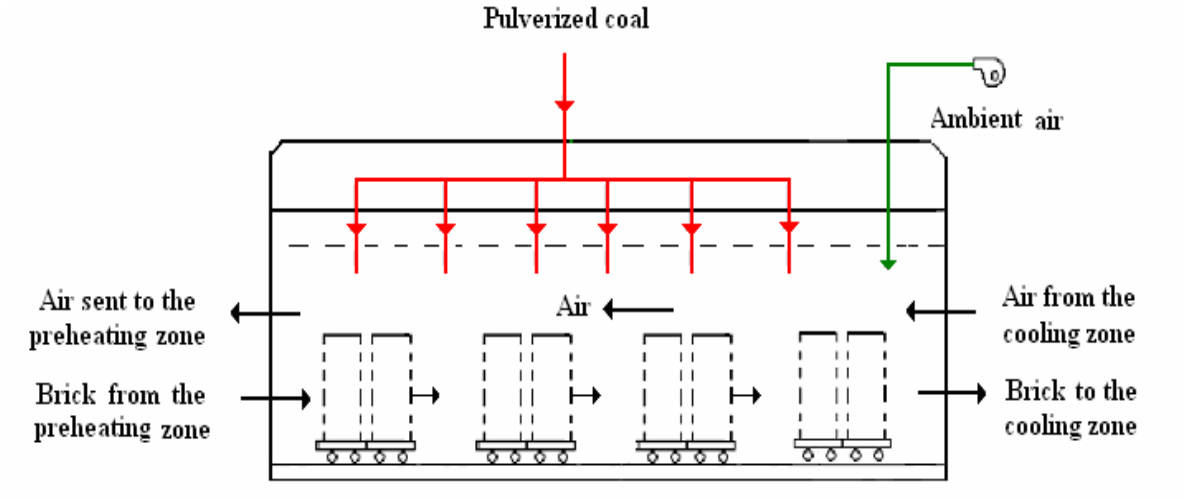

Figure VI.2 Schematic Representation of the Firing Zone

In the existing tunnel kiln the pulverized coal is added from 21 different holes along the firing zone. The total ratio of pulverized coal added is 0.0272 kg coal/kg brick. Similarly the secondary air is fed from 9 different points with a total flow rate ratio of 0.272 kg air/kg brick. In order to compare the tunnel kiln data the pulverized coal and secondary air flow rate ratios were considered to be distributed equally for the holes they are supplied as shown in Table VI.4. Then the pulverized coal and secondary air mass flow rate ratios are 0.0013 kg coal/kg brick and 0.0302 kg air/kg brick respectively for each hole.

In the preparation of the green bricks, the ratio of the admixed coal to brick mass was given as 0.206 on green brick basis. This ratio becomes 0.224 based on fired bricks. It was given that approximately the 20% of the admixed coal is carbon. Then the percentage of carbon coming from the admixed coal was given as 4.12 and 4.48% based on the green and fired bricks respectively. The data concerning the carbon percentage used in the green brick for the existing tunnel kiln was reported to be 4.34%.

TableVI.4 Fuel ndA ir Mass Flow Rate, Measured Temperatures along the Firing Zone of the Existing Tunnel Kiln

	In	T1-T5	B1	T6	T2	T7-T8	B3	T9-T10	B4	T11	B5	T12	B6	T13	B7	T14-T15	B8	T16	B9	T17-T21	Out
$\frac{\overline{L}}{\%}$	0	20-34	37	39	42	43-46	48	49-52	55	56	57	58	61	62	64	65-68	70	71	73	76-90	100
g_a^b			0.0302		0.0302		0.0302		0.0302		0.0302		0.0302		0.0302		0.0302		0.0302		
g_{pc}		5× 0.0013		0.0013		2× 0.0013		2× 0.0013		0.0013		0.0013		0.0013		2× 0.0013		0.0013		5× 0.0013	
G_a	1.12																				0.8
T_m		649-695		697		688-703		758-735		775		789		812		824-838				857-792	

The mass and energy balances were computed around the firing zone by using data collected from the industrial plant and the results were given in Table VI.5. At the entrance of the firing zone, kiln cars have a heat content of 887.4 kJ/kg brick while the brick loads have 819.3 kJ/kg brick. So in the solution of the model equations kiln cars can be considered as brick loads. In order to compensate the heat load of the kiln cars, the computations were done for a brick flow rate of 2.083 kg/m^2 s as basis. Hot air temperature from cooling to firing zone was calculated to be 800°C by using mass and energy balances, around the firing zone for the existing tunnel kiln.

Table VI.5 Mass and Energy Balances around the Firing Zone for Existing Tunnel Kiln

	Mass flow rate ratio (kg/kg brick)		Temperatures (^{o}C)		Heat flow rate ratio (kJ/kg brick)	
	In	Out	In	Out	In	Out
Hot air coming from the cooling	0.8		800		686.8	
Hot air from firing to preheating		1.12		690		872.2
Secondary air for combustion of	0.272		20		5.5	
Pulverized coal	0.045				826,4	
Admixed coal carbon	0.03				1003.2	
Bricks	1	1	600	980	501.6	819.3
Kiln cars	1.083	1.083	400	980	362.1	887.4
Heat loss						660.0
Top cooling air	0.86	0.86		100	0.0	86.7
Total Balance	**4.085**	**4.083**			**3385.0**	**3378.6**

VI.2 OPTIMIZATION OF THE COOLING ZONE

The model equations were used to find out the optimized values of the fresh air inlet flow rate, the suction and blowing air flow rates in order to minimize the total pressure drop. The state variables such as the air and brick temperatures, superficial air mass flow rate were also obtained at the end of the optimization. Variation of the air and brick temperatures together with the measured plant data were shown in Fig. VI.4 whereas the suction and blowing air flow rate profiles were shown in Fig. VI.5. The brick temperature decreases gradually from 980°C to 33°C along the cooling zone whilst the air temperature increases from the brick exit side towards the brick entrance side.

The measured temperatures given in Table VI.1 were compared to the brick and air temperatures obtained as a result of model based optimization in Fig. VI.3.

The measured temperatures from the cooling zone are practically values between the brick and air temperatures. In Fig. VI.3, all three results were plotted together to represent the variation of the temperatures along the kiln length.

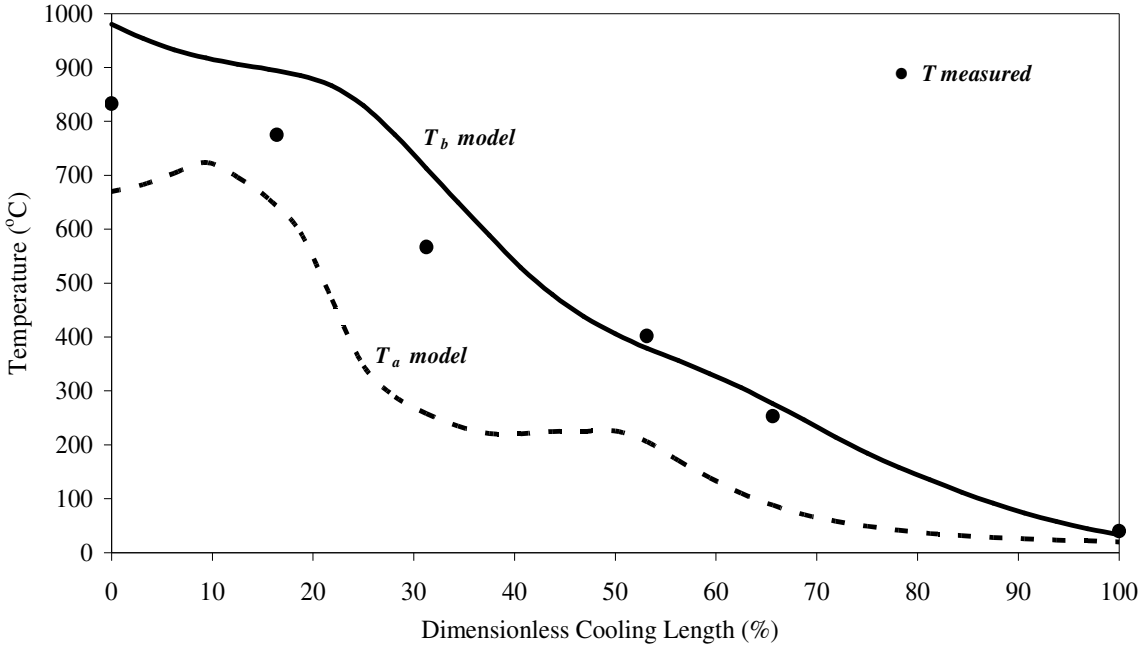

Figure VI.3 Measured Temperatures, Computed Air and Brick Temperatures

The superficial air mass flow rate together with the optimized suction and blowing air flow rates are plotted in Fig.VI.4. The line representing the suction or blowing air flow rate changes sign along the cooling zone. The values greater than zero represent the flow rate of the air being introduced into the kiln (blowing) while values less than zero indicate the flow rate of the air removed from the kiln (suction). The model based optimization of the cooling zone showed four different regions as being two regions of suction and two regions of blowing as shown in Fig. VI.4. The objective of blowing ambient air just at the very beginning of the cooling has two purposes such as increasing the temperature difference between the bricks and air and also to prevent back mixing which causes the leakage of the hot air from the firing to the cooling zone. The necessity of the null pressure line was reported to be one of the main concerns to regulate the stability of air flow in practice and in the literature as well Stamatis and Manesis (2005). There is another region of blowing of the ambient air right after the first suction line from the brick entrance side in order to increase the cooling rate.

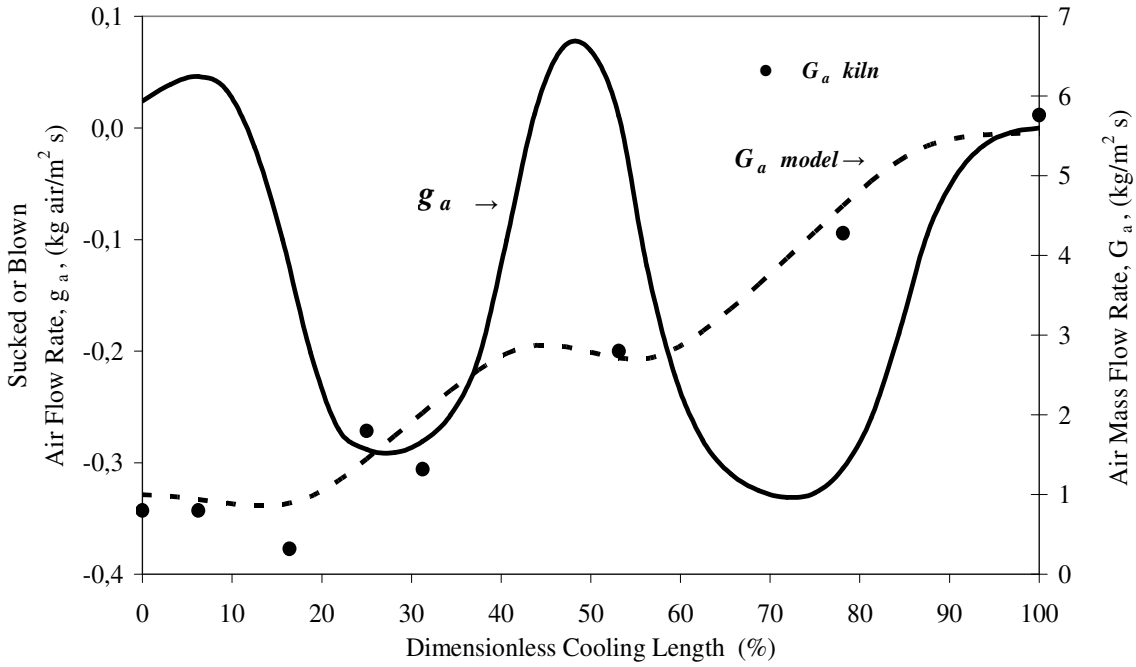

Figure VI.4 Superficial Mass Flow Rates of Suction, Blowing and Kiln Air Obtained by Optimization and Measurements

Table VI.6 Overall Mass Balance around the Cooling Zone for Plant Data and Optimization Results

	Mass flow rate (kg/m^{2}s)						Suction air temperature (°C)
	Inlet Air		Outlet Air		Total In	Total Out	
	Kiln exit	Blowing	Firing zone	Suction			
Optimization results	5.53	0.31	1.00	4.84	5.84	5.84	192.3
Cooling zone data	5.76	0.96	0.80	5.92	6.72	6.72	188-200

The air flow rate data obtained around the cooling zone of the tunnel kiln, Table VI.6, were compared with the optimized results. Similar to Table VI.2, the overall mass and energy balances obtained from the results of the model based optimization were given in Table VI.7. The results obtained around the system boundaries given by tables VI.6 and VI.7 gave results very close to those presented in Table VI.2 which is for the existing tunnel kiln. This shows that considering the heat content of the kiln cars as brick loads is a valid assumption.

According to the optimized results, Table VI.7, the total air flow rate circulating, 5.84 kg/m^{2}s, was estimated to be 15% lower than the existing tunnel kiln, 6.72 kg/m^{2}s. On the other hand, the air temperature from the cooling to firing zone was estimated to be 800°C using the measured plant data, Table VI.2, whereas

it was calculated to be 670°C as a result of the model based optimization along the cooling zone as shown in Fig. VI.3. The validity of the model can be checked by comparing tables VI.2, VI..6 and VI.7.

Table VI.7 Mass and Energy Balances around the Cooling Zone using the Results of the Model Based Optimization

	Mass flow rate ratio (kg/kg brick)		Temperatures (°C)		Heat flow rate ratio (kJ/kg brick)	
	In	Out	In	Out	In	Out
Inlet air from the tunnel kiln exit	5.53		20		113.7	
Air blown for cooling	0.31		20		6.3	
Air sucked for drying kiln		4.84		192.3		979.7
Hot air from cooling to firing		1.00		670.0		752.3
Bricks	1.00	1.00	980	33	823.2	23.5
Kiln cars	1.083	1.083	980	33	823.2	23.5
Total Balance	7.84	7.84			1766.4	1779.0

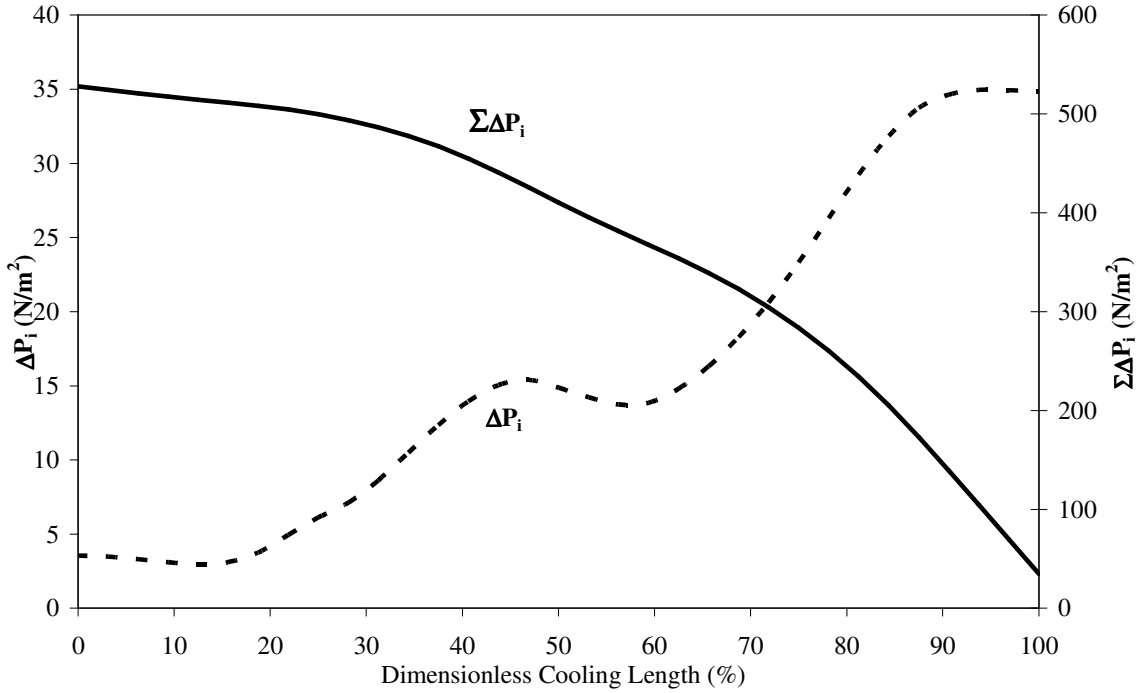

Figure VI.5 Total Pressure Drop and Pressure Drop for each Δx Element along the Cooling Zone

In Fig. VI.5, one can see the pressure drop, ΔP_i, for each Δx element and the total pressure drop, $\sum \Delta P_i$, as the air flows along the cooling zone. The total pressure drop curve, $\sum \Delta P_i$, is in fact the integration of the area under the curve giving the differential pressure drop, ΔP_i, at any distance. There are locations for measuring

the pressure in the cooling zone of the existing kiln. Using the measured plant data, the pressure drop along the cooling zone of the tunnel kiln was found to be varying between 500 and 600 N/m^2. This gives a satisfactory agreement with the computed results of model based optimization.

VI.3 OPTIMIZATION OF THE FIRING ZONE

In the present work, the optimal air flow rate required for complete combustion of the admixed and pulverized coal with the optimal air and pulverized coal feed locations were computed to minimize the fuel cost in the firing zone. When the model equations were solved, the air and the brick temperatures and optimal air flow rate were obtained as depicted in Fig.VI.6. As soon as the air from the cooling zone enters the firing zone, the air temperature starts to increase because of the contact of the air with the bricks at higher temperatures.

As shown in Fig.VI.7 pulverized coal is fed into the firing zone between the 18 % and % 95 of the firing zone length. It is seen that carbon percentage in the bricks (W_c) decreases gradually and becomes almost zero while reaching the 80 % of the dimensionless cooling length of the firing zone. Furthermore, between the about 30 % and 80 % of the firing zone length, secondary ambient air is fed into the firing zone.

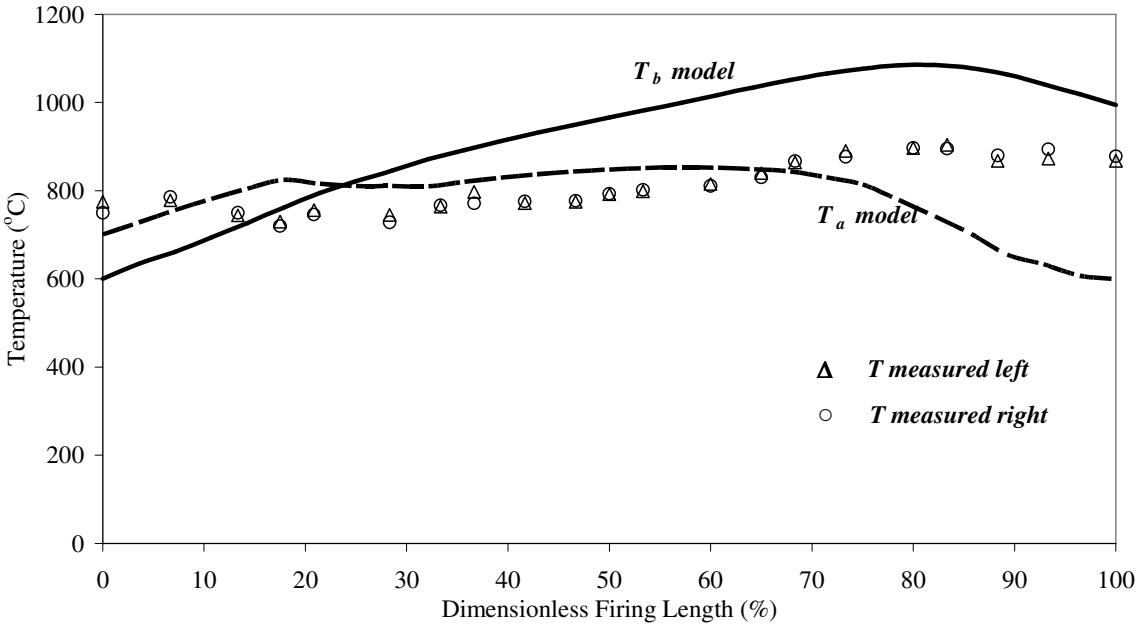

Figure VI.6 Comparison of the Measured Temperatures to the Computed Air and Brick Temperatures

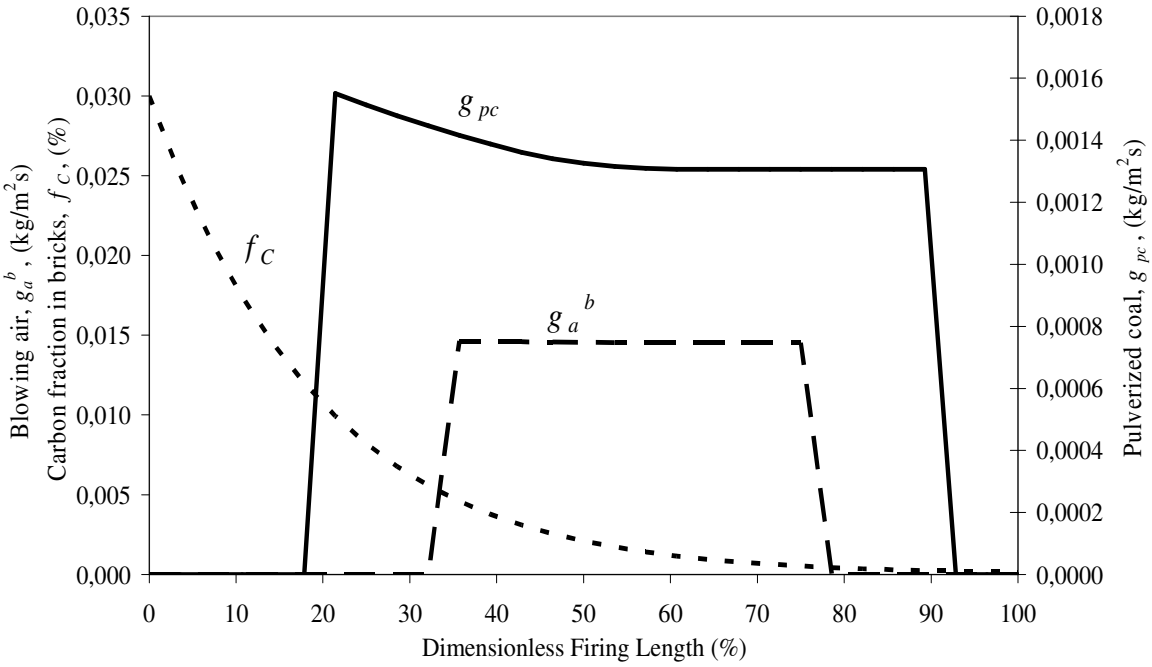

Figure VI.7 Profiles of the System Parameters along the Firing Zone

If we look at the air flow rate in Fig.VI.8, it stays constant for a while since there is no secondary air and/or pulverized coal fed into the firing zone until that length. There is gradual increase in the value of the superficial air mass flow rate in Fig.VI.8, as the secondary air and/or the pulverized coal start to be blown into the firing zone.

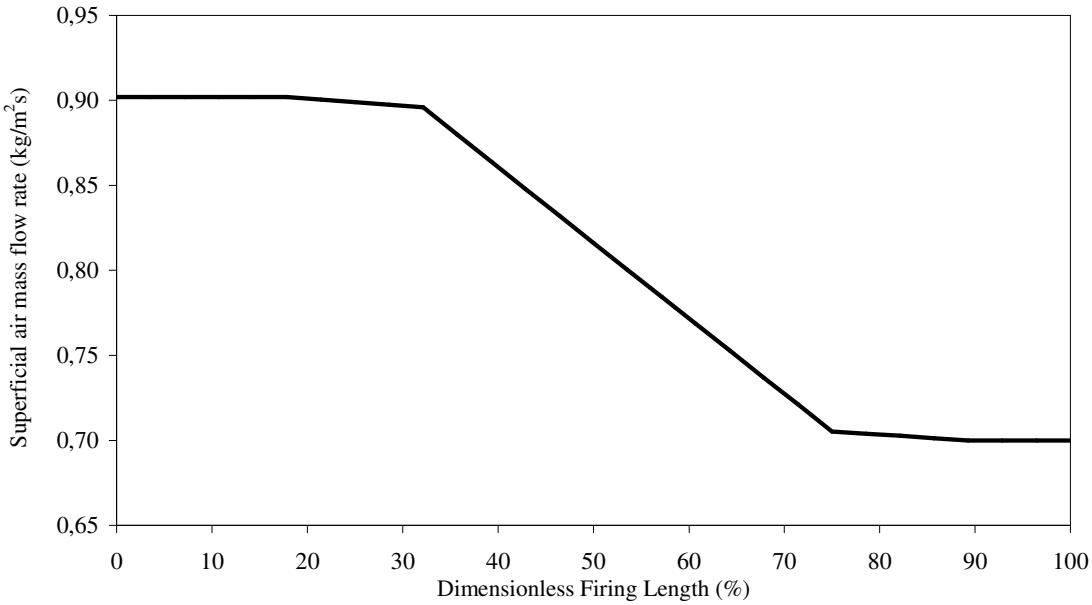

Figure VI.8 The Superficial Air Mass Flow Rate Along the Firing Zone

Composition of air changes throughout the firing zone. As a result of the combustion of pulverized and admixed coal, the oxygen concentration of the flowing air decreases gradually from 21% to 5% as shown in Fig. VI.9.

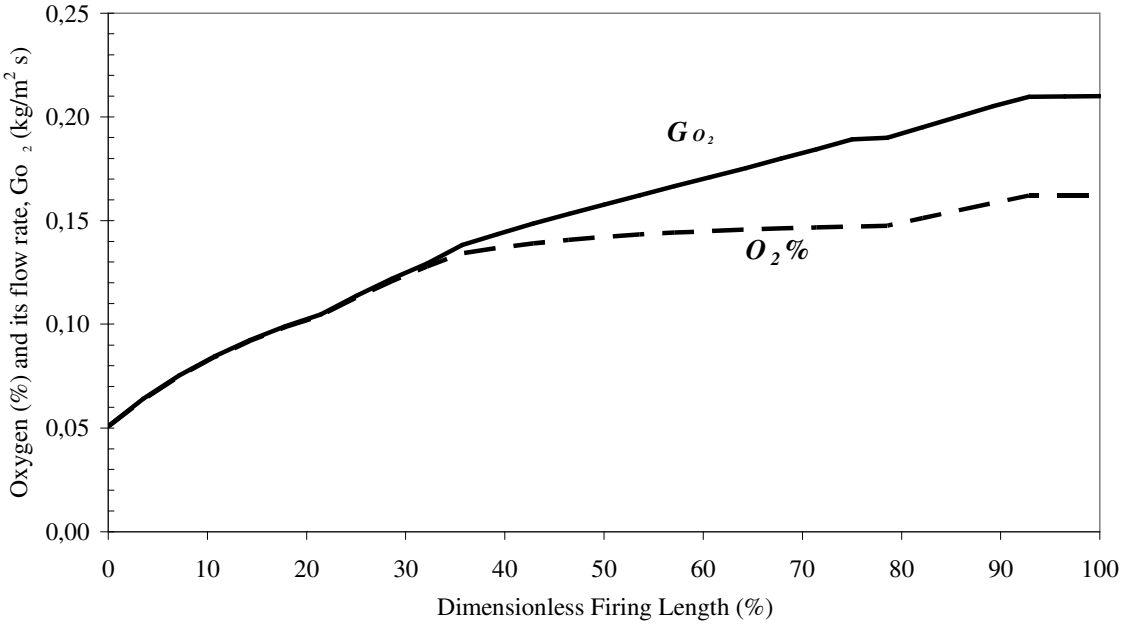

Figure VI.9 Superficial Mass Flow Rate and Percentage of Oxygen along the Firing Zone

As seen in Fig.VI.9 oxygen percentage ($\%O_2$) starts to decrease with the combustion of pulverize coal. Additionally, carbon combustion in the bricks brings about the decrease oxygen percentage and available oxygen as well.

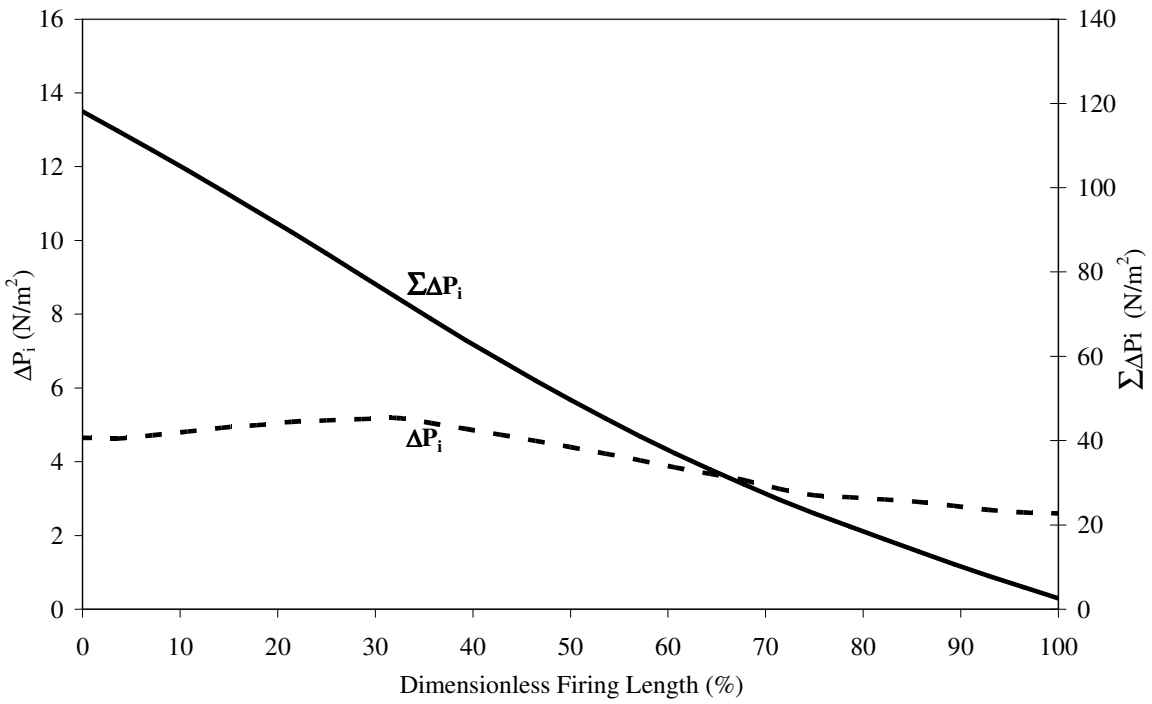

Figure VI.10 Total Pressure Drop and Pressure Drop for each Δx Element along the Firing Zone

As discussed in the cooling part, the pressure drop is affected considerably by the suction and blowing air flow rates together with the air density which is a function of air temperature along the cooling zone. Unlike the cooling zone, the incremental pressure drop in the firing zone does not represent fluctuations as shown by figures VI.5 and VI.10. Because there is no reduction in air flow rate caused by suctions in the firing zone and air flow rate increases continuously due to the blown air flow rate and coal combustion. Consequently, the pressure drop being parallel to the air flow rate shows changes as depicted in Fig.VI.8 and Fig.VI.10.

The results of overall mass and energy balances for firing zone using the optimized variables are illustrated in Table VI.8. The flow rate of the secondary air was found to be 0.175 kg/kg brick whereas the industrial data given in Table VI.5 was 0.272 kg/kg brick. It is advantageous to use lesser secondary air because secondary air has a cooling effect in the firing zone. The optimized values of the admixed and pulverized coal ratios were found to be 0.04 and 0.025 kg/kg brick respectively to give the minimum fuel cost.. The plant data for the admixed and pulverized coal ratios are 0.03 and 0.045 kg/kg brick.

Table VI.8 Mass and Energy Balances around the Firing Zone Using the Results of the Model Based Optimization

	Mass flow rate ratio (kg/kg brick)		Temperatures (^oC)		Heat flow rate ratio (kJ/kg brick)	
	In	Out	In	Out	In	Out
Hot air coming from the cooling	0.70		760		616.0	
Hot air from firing to preheating		0.96		650		730.3
Secondary air	0.175		20		3.8	
Pulverized coal	0.025				470.2	
Admixed coal carbon	0.04				1337.6	
Bricks	1	1	600	990	501.6	826.7
Kiln cars	1.083	1.083	400	990	362.1	896.3
Heat loss						660.0
Top cooling air	0.86	0.86		100		86.7
Total Balance	**3.886**	**3.903**			**3291.3**	**3200.0**

The average heating value of the admixed coal measured in the laboratory is 4541.58 kJ/kg coal as shown in Table VI.3 whereas in the existing plant this value was considered to be around 6449 kJ/kg coal. Similarly the heating value of the pulverized coal was measured as 16 874.67 kJ/kg coal while it was stated to be 18 441.20 kJ/kg coal for the pulverized coal used in the plant. The optimization of the flow rates of the pulverized coal, admixed coal and the secondary air was done using the measured heating values. According to the measured values the carbon content of the admixed coal is 13.6% based on the average heating value given in Table VI.3. Thus it is necessary to use more admixed coal as high as 0.294 kg coal/kg brick while keeping the carbon percentage in the bricks at 4%. The heating value of the pulverized coal was stated to be 18 441.20 kJ/kg coal. However the average measured heating value was found to be 16874.67 kJ/kg coal. The differences in the results of tables VI.5 and VI.8 are mainly due to the heating values in addition to amounts of pulverized coal, admixed coal and secondary air.

Table VI.9 Comparison of Plant Data and Optimization Results

	Inlet air flow rate (kg/m^2s)		Outlet air flow rate (kg/m^2s)	Total flow rate (kg/m^2s)		Coal mass flow rate		Fuel Cost (Euros/ton brick)
	Firing outlet	Blowing	Firing inlet	In	Out	Pulverized (kg/kg brick)	Admixed (%/kg brick)	Total
Optimization	0.7	0.175	0.96	0.875	0.96	0.025	0.04	1.17
Firing zone data	0.8	0.272	1.12	1.072	1.12	0.045	0.03	1.75

The costs of pulverized and admixed coals are 33.34 Euros/ton and 8.33 Euros/ton respectively. The total fuel cost was calculated using the tunnel kiln data

and the optimized results as given in Table VI.9. The difference in the fuel cost is 0.58 Euro/ton brick.

PART VII

CONCLUSION

It was reported in the 8th Five Year Development Plan of the State Planning Organization of Turkey that Turkey's annual brick production to be around 22 million tons. A very simple calculation based on an energy requirement of 2200 kJ/kg brick shows that the annual energy consumption for brick production will be around 4.84×10^{10} MJ. This shows that even a reduction of 1% in the energy consumption will reduce the annual energy requirement by 484.0×10^{6} MJ which is equal to 134.4×10^{6} MWh. This very simple calculation shows the importance of developing energy efficient operation of the energy intensive processes. As a comparison it is important to note that in the year 2004 Turkey's annual electricity energy consumption was reported to be 159.5×10^{6} MWh.

The research presented in this thesis addresses developing model based optimization techniques for cooling and firing zones of a tunnel kiln. The optimization was realized by considering the each zone as a decomposable structured system formed of N interconnected cells.

Using the mathematical model, the optimization was performed to minimize the pressure drop and improve heat recovery by finding the optimum values of the ambient air inlet flow rate, the suction and blowing air flow rate profiles along the cooling zone. The state variables such as the air and brick temperatures, superficial air mass flow rate were obtained after solving the objective function for minimum total pressure drop while satisfying the process constraints. The optimization results for cooling zone showed that:

- There should be four distinct regions formed of two sets of suction and two sets of blowing regions.

- Starting from the beginning of the cooling where the hot bricks leave the firing zone, the first 12% of the cooling zone is the first set of blowing to increase the heat transfer rate and to prevent back mixing of the hot air from the firing to the cooling zone.
- Following the first set of blowing, there is a region of suction between the 12% and 43% of the dimensionless cooling length for recovering the hot air to be used in the drying kiln.
- The second set of blowing is in the region which lies between 43% and 54% of the cooling zone.
- The second set of suction is in the region where most of the air is sucked. It starts at a distance of 54% and extends to the cooling zone exit.
- Flow rate and temperature of the total suction air were calculated to be 4.84 kg/m2 s and 192.3 ^{0}C.
- Fresh air is sucked into the kiln at cooling zone exit. This value was also optimized and compared to the reported plant data as shown in Table VI.4.

The present work gives a sound estimation of the heat transfer and fluid flow phenomena and the optimum operating conditions in the cooling zone of a tunnel kiln. The approach presented here can also be extended to simulate the cooling zone of tunnel kilns producing ceramic wares. Optimal operating conditions for efficient heat recovery can be investigated by performing simulations for different kiln design.

The objective function of the firing zone is the fuel cost. The developed model equations for minimum fuel cost were solved by finding the optimal flow rate of the pulverized coal, admixed coal within the bricks in addition to flow rate of the secondary air fed from top of the kiln. The optimal air flow rate was calculated for complete combustion of the admixed and pulverized coal combustion. The optimization results were tested by using the plant data. As a result, for minimum fuel cost, it was found that:

- Carbon percentage in the bricks, f_C, becomes zero at about the 80 % of the dimensionless cooling length of the firing zone.
- Secondary ambient air is fed into the firing zone between the about 30 % and 80 % of the firing zone length.

- The flow rate of the secondary air was found to be 0.175 kg/kg brick that is smaller than the existing air flow rate. Consequently, undesired cooling effect caused by the secondary air fed into the firing zone will be smaller.
- The optimized value of the pulverized coal was found to be lower than the existing tunnel kiln. This makes a certain decrease in the plant operating cost when based on yearly production. Turkey's annual brick production was stated to be 22 million tons (DPT: 2530-ÖİK: 546, 2000) which shows that there may be a saving of 12.76×10^6 Euros annually.
- If the carbon percentage in the brick body is kept constant as 4 %, more admixed coal must be used to obtain minimum fuel cost.

As a result, heating values of admixed coal and pulverized coal are the key parameters to obtain minimum fuel cost. When the carbon percentage of the admixed coal in the brick body is increased in the permissible limits, this will reduce the amount of the pulverized coal fed into the firing zone, as well as fuel cost.

REFERENCES

[1] Abdelghani-Idrissi, M. B., Bagui, F. and Estel, L., "Analytical and experimental response time to flow rate step along a counter flow double pipe heat exchanger", International Journal of Heat and Mass Transfer 44 **(2001)** 3721-3730.

[2] Abou-Ziyan, H. Z. "Convective heat transfer from different brick arrangements in tunnel kilns", Applied Thermal Engineering, 24 **(2004)** 171-191.

[3] Aziz, N., and Mujtaba, I. M., "Optimal operation policies in batch reactors", Chemical Engineering Journal 85 **(2002)** 313-325.

[4] Callister, W. D., Materials Science and Engineering, 6th edition, John Wiley and Sons, **(2003)**.

[5] Caputo, A. C. and Palaggage, P. M., "Economic design criteria for cooling solid beds", Applied Thermal Engineering 21 **(2001)** 1219-1230.

[6] Caputo, A. C. and Palaggage, P. M., "Heat recovery from moving cooling beds: transient modeling by dynamic simulation", Applied Thermal Engineering 19 **(1999)** 21-35.

[7] Chapra, S. C. and Canale, R. P., Numerical Methods for Engineers, Mc Graw Hill, New York **(2002)**.

[8] Collin, M and Rowcliffe, D. Analysis and prediction of thermal shock in brittle materials, Acta Materialia, 48 **(2000)** 1655-1665.

[9] Dugwell, D. R. and Oakley, D. E., A model of heat transfer in tunnel kilns used for firing refractories, Int. J. Heat Mass Transfer, 31, **(1988)** 2381-2390.

[10] Dugwell, D. R. and Oakley, D. E., "Simulation of tunnel kilns for firing refractory products", Br. Ceram. Trans. J., 86, **(1987)** 150-153.

[11] Essenhigh, R. H., and Mescher, M. A., "Mechanism of carbon combustion: Relative influence of adsorption, desorption, and boundary layer diffusion as a function of pressure", The Combustion Institute 111:350-352 **(1997)**.

[12] Förtsch, D., Schnell, U. and Hein, K. R. G., "The mass transfer coefficient for the combustion of pulverized carbon particles", The Combustion Institute 126:1662-1668 **(2001)**.

[13] Geankoplis, C. J., Transport processes and separation process principles, Prentice-Hall, **(2003)** 93-100.

[14] Halasz, G., Toth, J. and Hangos, K. M., "Energy optimal operation conditions of a tunnel kiln", Comput. Chem. Engng, 12, **(1988)** 183-187.

[15] Hilmer, F., Vajen, K., Ratka, B., Beckermann, H., Fuhs, W. and Melsherimer, O., "Numerical solution and validation of a dynamic model of solar collectors working with varying flow rate", **(1998)** PII: S0038-092X(98)00142-X.

[16] Holman, J. P., Heat Transfer, 9 th edition, Mc Graw-Hill, New York (**2001**).

[17] Incropera, Frank P.; Dewitt, David P.; Introduction to Heat Transfer, Third Edition, John Wiley & Sons, (**1996**).

[18] Iwanaga, M. and Takatani, Mathematical model analysis for oxidation of coke at high temperature, Iron and Steel Inst. Japan, 29 **(1989)** 43-48.

[19] Junge, K., Energy demand for the production of bricks and tiles, Ziegelindustrie International, Number 4 **(2002)** 16-24.

[20] Mancuhan, E. and Kucukada,K., "Optimization of fuel and air use in a tunnel kiln to produce coal admixed bricks", Applied Thermal Engineering, available online, 26 **(2006)** 1556-1563.

[21] Panagiotis, M. and Stamatis, M. "Modelling and control of industrial tunnel-type furnaces for brick and tile production", Proceeding of the 5th International Conference on Technology and Automation, Thessaloniki, Greece, **(2005)** 216-221.

[22] Prasertan, S., Theppaya, T., Prateepchaikul, G. and P. Kirirat, "Development of an energy-efficient brick kiln", International Journal of Energy Research, **(1997)** 1363-1383.

[23] Punbusayakul, N., Charoensuk, J. and Fungtammasan, B., "Modified sulfation model for simulation of pulverized coal combustion", Energy Conversion and Management 47 **(2006)** 253-272.

[24] Ray, W. H. and Szekely, J., Process Optimization, Jonh Wiley and Sons, New York, **(1973)** 157-211.

[25] Smith, I. W., "The intrinsic reactivity of carbons to oxygen", Fuel, 57 **(1978)** 409-414.

[26] Theppaya, T., Prasertan, S., Prateepchaikul, G., Saensabai, P., and Kirirat, P., "Design, construction and test run of an energy-efficient brick kiln", in: The 5th ASEAN Science and Technology week Scientific Conference on Non Conventional Energy Research, **(1998)** 175-180.

[27] Vogt, S. and Vogt, R., "On the modeling of firing curves to comply with quality standards (Part 1)", Ziegelindustrie International, Number 7 **(2004)** 20-35.

[28] Weber et al., "On the (MILD) combustion of gaseous, liquid, and solid fuels in high temperature preheated air", Proceedings of the Combustion Institute 30 **(2005)** 2623-2629.

[29] Wozny, G. and Li, P. "Planning and optimization of dynamic plant operation", Applied Thermal Engineering 20 **(2000)** 1393-1407.

[30] State Planning Organization, 8th Five Year Development Plan, Special report on stone and soil based products: Brick, tile, prefabricated construction materials, DPT: 2530-ÖİK: 546, **2000**[in Turkish].

[31] S. Peker, S.S. Helvaci, Fluid Mechanics: Concepts, Problems and Applications, Literatur Press, Istanbul **(2003)** (in Turkish).

APPENDIX A

MODEL EQUATIONS IN DISCRETIZED FORMS

A.1 COOLING ZONE

Equation (V.3) can be rewritten to represent the energy balance for the air flow in discretized form as a series of interconnected cells with the suction and blowing air being the optimization variables for each cell.

$$\left\{G_a C_{p_a} T_a\right\}\Big|_x = \left\{G_a C_{p_a} T_a\right\}\Big|_{x+\Delta x} + \left\{h_b a_b (T_b - T_a)\right\}\Big|_{x+\Delta x}\Delta x - \left\{h_w a_w (T_a - T_w)\right\}\Big|_{x+\Delta x}\Delta x + \left\{g_a^b C_{p_a} 20^o C \text{ or } g_a^s C_{p_a} T_a\right\}\Big|_{x+\Delta x} \quad \text{(A.1.1)}$$

Similarly, Eq. (V.5) can also be written in discretized form to present the brick temperature at a length of $x+\Delta x$:

$$G_b C_b T_b\Big|_{x+\Delta x} = G_b C_b T_b\Big|_x - \left\{h_b a_b (T_b - T_a)\right\}\Big|_x \Delta x - F_{bw}\sigma\varepsilon a_w \left(T_b^4 - T_w^4\right)\Big|_x \Delta x \quad \text{(A.1.2)}$$

Using above temperature gradient Eq. (V.7) can be rewritten as an implicit discretized equation to predict the wall inside temperature at a length of x is as follows:

$$T_w^4\Big|_x = T_b^4\Big|_x + \frac{1}{F_{bw}\sigma\varepsilon a_w}\left\{h_w a_w (T_a - T_w)\right\}\Big|_x \quad \text{(A.1.3)}$$

There are four unknowns, $T_a(x)$, $T_b(x)$, $T_w(x)$ and $G_a(x)$, and one objective function which should be solved simultaneously using equations (A.1.1), (A.1.2), (A.1.3). The optimization variables are the flow rates of the suction or blowing air flow rates, $g_a(x)$, and the inlet ambient air at the brick exit side $G_a(L)$.

A.2 FIRING ZONE

The energy balance for air in decomposed form for a length element of Δx can be written as:

$$\left\{G_a C_{p_a} T_a\right\}\Big|_x = \left\{G_a C_{p_a} T_a\right\}\Big|_{x+\Delta x} + \left\{h_b\, a_b\, (T_b - T_a)\right\}\Big|_{x+\Delta x} \Delta x - \left\{h_w\, a_w (T_a - T_w)\right\}\Big|_{x+\Delta x} \Delta x + \left\{g_a^b C_{p_a} 20^o C\right\}\Big|_{x+\Delta x} + \left\{g_{pc} \Delta H_{pc}\right\}\Big|_{x+\Delta x}$$

(A.2.1)

$$G_b C_b T_b\Big|_{x+\Delta x} = G_b C_b T_b\Big|_x - \left\{h_b\, a_b (T_b - T_a)\right\}\Big|_x \Delta x - F_{bw} \sigma \varepsilon a_w \left(T_b^4 - T_w^4\right)\Big|_x \Delta x + G_b \Delta H_{ac} \Delta f_C\Big|_x$$

(A.2.2)

The change of O_2 concentration along the length element, Δx:

$$MW_{O_2}\left[\frac{G_a(x+\Delta x) C_{O_2}(x+\Delta x)}{\rho_a(x+\Delta x)} - \frac{G_a(x) C_{O_2}(x)}{\rho_a(x)}\right] = -\left[g_{pc}(x) f_{C_{pc}} + G_b\left(f_C(x) - f_C(x+\Delta x)\right)\right]\frac{MW_{O_2}}{MW_C}$$

(A.2.3)

The change in the concentration of O_2 is directly proportional to the change of CO_2 concentration along the firing zone. Similarly this equation can be written in decomposed form.

$$-MW_{CO_2}\left[\frac{G_a(x+\Delta x) C_{CO_2}(x+\Delta x)}{\rho_a(x+\Delta x)} - \frac{G_a(x) C_{CO_2}(x)}{\rho_a(x)}\right] = MW_{O_2}\left[\frac{G_a(x+\Delta x) C_{O_2}(x+\Delta x)}{\rho_a(x+\Delta x)} - \frac{G_a(x) C_{O_2}(x)}{\rho_a(x)}\right]$$

(A.2.4)

A.3 HEAT TRANSFER COEFFICIENT

The magnitude of heat transfer coefficient depends on the physical properties of fluid, the fluid flow rate and the physical arrangement of the heat transfer surface. Convective heat transfer coefficient can be calculated using the following correlations from Holman (2003).

$Nu = 0.332\, Re^{1/2}\, Pr^{1/3} \qquad 0.6 \le Pr \le 50 \quad Re \le 2100$

$Nu = 0.0308\, Re^{4/2}\, Pr^{1/3} \qquad 0.6 \le Pr \le 60 \quad Re \ge 2100$

$Nu = \frac{h\ D_e}{k_a}$, $Re = \frac{G_a\ D_e}{\mu_a}$ and $Pr = \frac{C_{p\,a}\ \mu_a}{k_a}$.

The Reynolds number is a quantity, which is used to estimate if the flow is laminar or turbulent. This is important, because increased mixing and shearing exist in turbulent flow. This gives rise to a higher heat transfer coefficient, which affects the efficiency of heat recovery.

APPENDIX B

PROPERTIES OF AIR AND BRICK

Thermal properties of were obtained after fitting the best curve for the data taken from Holman (2001). In the correlations given in Table B.1, temperature, T, is in K.

Table B.1 Properties of air

ρ_a (kg/m^3)	$2\times10^{-12}T^4 - 9\times10^{-9}T^3 + 1\times10^{-5}T^2 - 0.0097T + 3.056$
c_{pa} (J/kg °C)	$5\times10^{-6}T^2 + 0.2T + 944.9$
k_a (J/m s °C)	$4\times10^{-8}T^3 - 1\times10^{-4}T^2 + 0.14T - 6.41$
$\mu_a \times10^{-7}$ (Pa s)	$1\times10^{-7}T^3 - 4\times10^{-4}T^2 + 0.68T + 11.97$

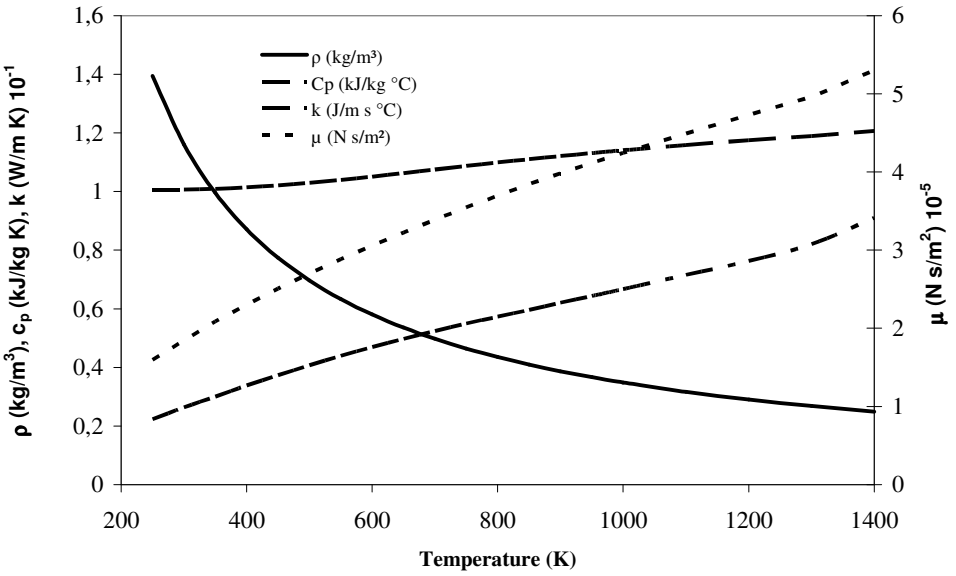

Figure B.1 Variation of Air Properties with Temperature

Table B.2 Properties of Brick

ρ_b (kg/m^3)	1600	Holman (2003)
C_b (J/kg °C)	836.4	Holman (2003)
k_b (J/m s °C)	0.85	Holman (2003)
e (-)	0.93	Holman (2003)
α_T (1/°C)	5.5-11×10^{-6}	Vogt and Vogt (2004), Collin and Rowcliffe (2000)
σ_T (MPa)	50-100	Vogt and Vogt (2004), Collin and Rowcliffe (2000)
E (GPa)	6-10	Vogt and Vogt (2004), Collin and Rowcliffe (2000)

APPENDIX C

C.1 FRICTION FACTOR

The correlation giving the friction factor, *f,* also known as Wood equation, was taken from Peker and Helvaci (2003):

$$f = a + b\,Re^{-c} \qquad \text{for } Re > 2300$$

where,

$$a = 0.0235\left(\frac{\varepsilon}{D_e}\right)^{0.225} + 0.1325\left(\frac{\varepsilon}{D_e}\right)$$

$$b = 0.0235\left(\frac{\varepsilon}{D_e}\right)^{0.44} \quad and \quad c = 0.0235\left(\frac{\varepsilon}{D_e}\right)^{0.134}$$

C.2 EFFECT OF SPACING ON THE AIR FLOW

In this considered system, the pressure drop occurs due to the flow of air through the holes of the brick and through the spacing between brick packages. In the case of constant potential and kinetic energy for a system, pressure drop is only equal to the energy loss due to the friction. The most important thing to note here about friction is that it is independent of the surface area in contact. Therefore, pressure drop due to the friction is the same for each branch in parallel-connected pipes whatever the cross sections are. The air flow throughout the tunnel kiln was considered to be similar to the flow of fluids in parallel pipes so that the flow rates through the brick and spacing are different but the pressure drop through either bricks or spacing is the same. The reason is that, it is split into many branches through the brick holes and spacing between the packages. Consequently, pressure drop in brick holes will be equal to the pressure drop throughout the spacing between packages and equal to the total pressure drop along the cooling zone as well.

The real density of bricks varies between 1600 and 1400 kg/m^3 but the bricks with horizontal holes have an apparent density of 600 kg/m^3 while the bricks with vertical holes have densities around 700 and 800 kg/m^3. According to this information, the range of the void fraction and also the flow area fraction of bricks can be predicted.

$$\rho_b = \text{Real density} = \frac{\text{Brick mass}}{\text{Brick volume}} \tag{C.1}$$

$$\rho_b^* = \text{Apparent density} = \frac{\text{Brick mass}}{\text{Total volume}} \tag{C.2}$$

$$\frac{\rho_b^*}{\rho_b} = \frac{\text{Brick volume}}{\text{Total volume}} = \frac{V_b}{V_T} = \frac{V_T - V_b}{V_T} = 1 - \frac{V_o}{V_T} \tag{C.3}$$

Hence, the fraction of the empty volume $\frac{V_O}{V_T}$ is found as

$$\frac{V_o}{V_T} = 1 - \frac{\rho_b^*}{\rho_b} \tag{C.4}$$

If the flow length for the bricks is considered as L, the fraction of flow area can be defined as follows:

$$\frac{V_O}{V_T} = \frac{A_O L}{A_T L} \tag{C.5}$$

and

$$\frac{A_0}{A_T} = 1 - \frac{\rho_b^*}{\rho_b} \tag{C.6}$$

This relation is used to predict the flow area within the bricks.

There are four brick packages and the two of them have a width of 1.7 m and the other two have a width of 1.9 m. The total width of the kiln is 8.1 m. Then the spacing along the width is 0.9 m. The spacing between the brick packages is 0.2 m while the spacing between the kiln walls and brick packages is 0.15 m. Approximately the fraction of the flow area can be found as

$$\frac{A_o}{A_T} = 1 - \frac{700}{1200} = 0.42$$

Furthermore, the dimensions of the kiln and brick packages will be used to find the flow area outside the bricks.

The percentages of the areas occupied by different elements of the tunnel kiln are given by Tables C.1 and C.2.

Table C.1 Areas Occupied by Different Elements of the Tunnel Kiln

	Area (%)
Brick packages	60.36
Spacing between the brick loads	5.03
Spacing between the brick loads and kiln walls	2.50
Area under the kiln cars	6.24
Area between two kiln cars	1.87
Area on top of the brick loads	4.33
Remaining area (mainly kiln cars)	19.67
Total kiln area	100

Table C.2 Distribution of Brickmaking Areas of the Tunnel Kiln

	Area (%)	**Corrected Percent Area (%)**
Brick packages	60.36	83.58
Spacing between the brick loads	5.03	6.96
Spacing between the brick loads and kiln walls	2.50	3.46
Area on top of the brick loads	4.33	6.00
Total brickmaking area	72.22	100

The total brickmaking area defined in Table C.2 is defined as the area above the kiln cars. The values given in Table C.2 are used to calculate the effect of spacing on the total flow rate. An equivalent diameter of 4 cm for the bricks and 40 cm for the spacing was used to calculate the superficial mass flow rate versus pressure drop curves given by Fig. C.1. Brick packages and spacing can be considered as flow in parallel pipes. The curves are used to find the flow rates for the same differential pressure drops. Table C.3 was prepared to show the effect of the air flowing through the spacing on the total flow rate. It is advantageous to decrease the spacing area in order to use efficiently the air flowing through the kiln.

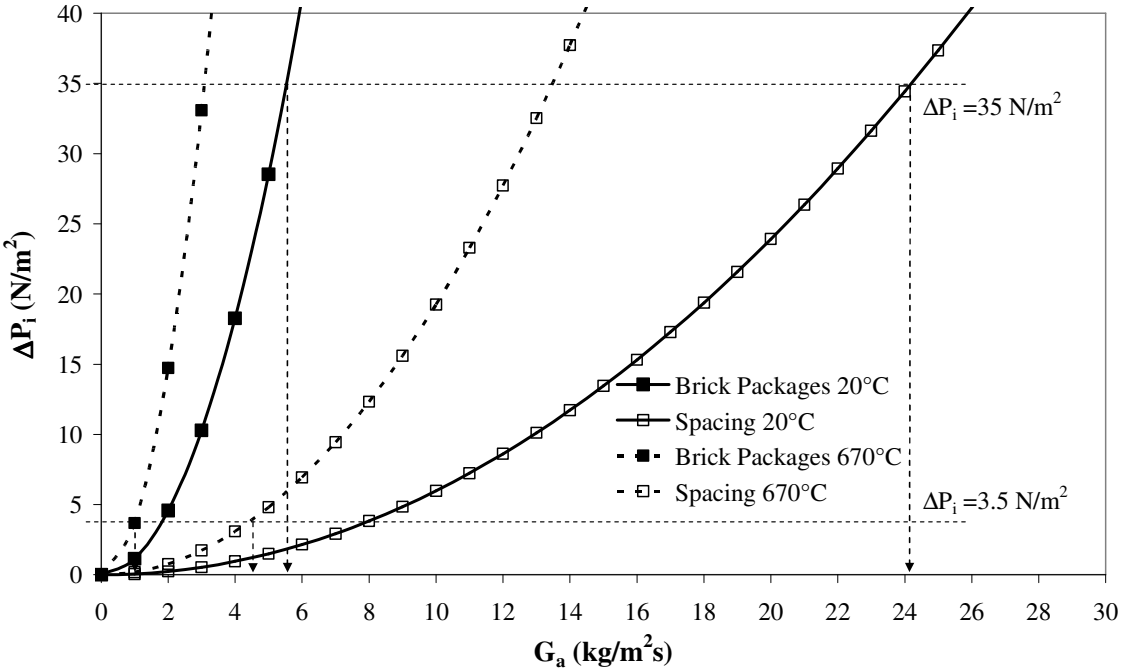

Figure C.1 Pressure Drop for Δx Length Element on both Ends of the Cooling Zone

Table C.3 Superficial Mass Flow Rate Distribution on both Ends of the Cooling Zone

	ΔPi (N/m^2)	T_a (°C)	Flow Rate, G_a, (kg/m^2s)		
			Brick (83.6%)	Spacing (16.4%)	Total (100%)
Brick Out	35	20	5.5	24.1	8.55
Brick In	3.5	670	0.9	4.4	1.47

APPENDIX D

KINETICS OF ADMIXED COAL COMBUSTION

$$-\frac{dC_C}{dt} = k\, a_{C_0} f_C^{2/3}\, C_{O_2} \tag{D.1}$$

When the rate of carbon consumption is written in terms of brick mass flow rate and carbon percentage in bricks, the Eqn. (D.1) takes the following form:

$$\frac{dC_C}{dt} = \frac{1}{MW_C}\frac{dC_C}{dx}\frac{dx}{dt} = \frac{1}{MW_C}\frac{d(\rho_b f_C)}{dx} v_b = \frac{G_b}{MW_C}\frac{df_C}{dx} \tag{D.2}$$

When Eqn. (D.1) is substituted into Eqn. (D.2), because of the constant G_b throughout the firing zone, Eqn.(D.3) becomes as follows:

$$-G_b \frac{d\, f_C(x)}{dx} = k(x) a_{C_0} f_C^{2/3}(x)\; C_{O_2}(x) \tag{D.3}$$

The change of O_2 concentration along the length element, Δx:

$$\frac{d(G_a C_{O_2} / \rho_a)}{dx} = -\left[f_{pc} \frac{dg_{pc}}{dx} + G_b \frac{df_{ac}}{dx} \right] \frac{1}{MWc} \tag{D.4}$$

The change in the concentration of O_2 is directly proportional to the change of CO_2 concentration along the firing zone.

$$-MW_{CO_2} \frac{d\left(G_a C_{CO2} / \rho_a\right)}{dx} = MW_{O_2} \frac{d\left(G_a C_{O2} / \rho_a\right)}{dx} \tag{D.5}$$

AUTOBIOGRAPHY

I was born in 05.10.1981 in Lüleburgaz. After I had grduated from Lüleburgaz Super High School at 1999, I got started studying chemical engineering at Ege University. Then I started master in science at Marmara University Chemical Enginnering Department at 2004. and now I am working in Sanifoam Sunger Sanayi ve Ticaret A.S. as a reseach and development engineer.